Large scale excitations in disordered systems

LARGE SCALE EXCITATIONS IN DISORDERED SYSTEMS

MARTA SALES PARDO
Departament de Física Fonamental
Facultat de Física
Universitat de Barcelona
Diagonal 647
08028 Barcelona

Universitat de Barcelona
Barcelona

Programa de Doctorat
Física Avançada, bienni 1998-2000

Memòria presentada per na Marta Sales Pardo per optar al títol de
Doctor per la Universitat de Barcelona

Certifico que la present tesi doctoral ha estat realitzada sota la meva direcció.
Barcelona, octubre del 2002.

Fèlix Ritort Farran
Professor Titular
Departament de Física Fonamental
Universitat de Barcelona

Als meus pares,
al Ger,

Contents

Agraïments

Els agraïments sempre són la part més gratificant d'una tesi, en particular perquè significa que ja s'ha acabat. Fer una tesi no és una feina d'una sola persona i no l'hagués pogut dur a terme sense l'ajut i el suport de molta gent. Voldria agrair a totes les persones que durant quatre anys han fet més fàcil i agradable la meva feina.

La meva vida científica és encara molt curta i espero que sigui encara molt més llarga. Voldria començar aquests agraïments donant les gràcies a les dues persones que ho han fet possible. En primer lloc, el meu director de tesi, en Fèlix Ritort i Farran qui no només m'ha dirigit sinó que també ha fet tot el possible per ensenyar-me a ser un bon investigador i transmetre'm l'entusiasme per la ciència. Gràcies perquè sense el teu ajut aquesta tesi no hauria estat possible. En segon lloc, m'agradaria donar les gràcies a la persona que em va introduir en el el món de la recerca, en Javier Tejada Palacios. Tot i que el meu pas pel seu grup va ser curt, a ell li he d'agrair que m'ensenyés que la curiositat i la motivació no s'han de perdre mai.

A part de la vessant científica, l'entorn humà és un dels aspectes primordials. Tots sabem que els cafès i les pauses diàries són el moment més esperat quan no et surt res. Molt especialment vull agrair a l'Anna i a l'Adan la seva constància i les seves inestimables converses a tots els nivells. Per descomptat, ells no són els únics amb qui he compartit cafès i, per tant, són molts a qui m'agradaria esmentar (espero no deixar-me a ningú!), el Deibit, la Sònia, l'UBXlab en ple (tant els que hi són, Joan Manel, Roger, Neus, Toni, Marc, Merche com els que han marxat, Jordi, Manel, Francesc, Enrique, Chema, Elena), els fisikets (molt especialment la Cesca, el Sergio, l'Esther), tota la tropa de Planta Tres (Napo, Jan, Montse, Fèlix, Maria) i la de Planta Cinc (David -gracias por tu insistencia-, el Xavi, el M!quel, el Tomàs, l'Ivan, el Pablo, el Mateu, el Jose i com no l'Emma -sense tu els meus seminaris serien ciència ficció- i és clar en Manel Parra -la teva nevera és un dels encerts del departament-).

Una altre punt important és l'entorn físic de treball, és a dir el despatx pròpiament dit. He de dir que en aquest aspecte he estat privilegiada, he pogut gaudir de la llum del sol i he tingut molts companys que m'han ajudat, l'Oleg, l'Alberto Saa, el Nikolai i sobretot la Carmen. A ella li he d'agrair la companyia, l'ajut i, sobretot, les xerrades i els consells

que m'han donat, que són un dels petits tresors que m'emporto. Agrair també la seva disposició i el seu ajut a la resta de professors del departament, l'Ignasi, el Conrad, el Miquel Rubí, el Xavier Batlle, el Jesús González ... així com la seva part administrativa sense la qual una tesi no es pot llegir. Gràcies Olga, Carme i Rosa, i tambeé gràcies Jaume pel suport logístic.

També m'agradaria agrair tots els que han col·laborat o simplement interactuat amb mi en algun punt de la meva vida científica. Molt especialment el Hajime Yoshino, l'Enzo Marinari, l'Andrea Crisanti, el Jean-Philippe Bouchaud i el Marco Picco.

Per últim, el que més he d'agrair és el suport principalment afectiu que he rebut des de fora. No tinc paraules per expressar tota la meva gratitud. Al Domènec per fer que la meva tesi sigui maca. A la Sandra, la Miriam i la Isabel, per viatjar (i confiar) en mi, a la Peque (per ajudar-me i per fer-me riure.. i per comprar-me un Xin-Xan!), al Víctor i la Grace , als meus avis. Per últim el més important, els meus pares pels consells i pel seu suport incondicional que sé que tindré sempre i, sobretot el Ger, perquè creu en mi.

Abbreviation List

AT	Almeida-Thouless
a.c.	alternating current
EA	Edwards-Anderson
DP	Directed Polymer
DPRM	Directed Polymer in Random media
DW	Domain Wall
FBC	Free Boundary Conditions
FC	Field Cooled
FDT	Fluctuation-Dissipation Theorem
FM	Ferromagnetic
FSS	Finite Size Scaling
IRM	Isothermal-Remanent Magnetisation
MC	Monte Carlo
MK	Migdal-Kadanoff
MFT	Mean Field Theory
nn	nearest neighbours
nnn	next nearest neighbours
OPF	Order Parameter Fluctuations
PM	Paramagnetic
PBC	Periodic Boundary Conditions
RE	Replica Equivalence
REM	Random Energy Model
REEM	Random Energy Exponential Model
RG	Renormalization Group
RS	Replica Symmetry
RSB	Replica Symmetry Breaking
SK	Sherrington-Kirkpatrick
SG	Spin Glass
TRM	Thermo-Remanent Magnetisation
TRS	Time Reversal Symmetry
ZFC	Zero Field Cooled

Publications

The contents of this thesis are based on the following articles:

Published papers:

M. Sales and H. Yoshino, *Fragility of the free-energy landscape of the DPRM*, Phys. Rev. B **65**, 066131 (2002).

M. Sales and J-P. Bouchaud, *Rejuvenation in the Random-energy model*, Europhys. Lett **56**, 181 (2001).

F. Ritort and M. Sales, *Scaling approach to order-parameter fluctuations in disordered frustrated systems*, J. Phys. A: Math. Gen. **34**, L333 (2001).

M. Picco, F. Ritort and M. Sales, *Order Parameter fluctuations (OPF) in spin glasses: Monte Carlo simulations and exact results for small sizes*, Eur. Phys. J. B **19**, 565 (2001).

F. Ritort and M. Sales, *A conjectured scenario for order-parameter fluctuations in spin glasses*, J. Phys. A: Math. Gen. **33**, 6505 (2000).

Submitted articles,

M. Sales, J-P. Bouchaud and F. Ritort, *Temperature shifts in the Sinai model: static and dynamical effects*, - submitted to J. Phys. A: Math and Gen.

M. Picco, F. Ritort and M. Sales, *Random energy levels and low-temperature expansions for spin glasses*, - submitted to EPJ B.

M. Picco, F. Ritort and M. Sales, *Statistics of lowest excitations in two-dimensional Gaussian spin glasses*, - submitted to Phys. Rev. B.

Preface

The secret of getting ahead is getting started.
The secret of getting started is breaking your complex
overwhelming tasks into small manageable tasks,
and then starting on the first one.

Mark Twain

The analysis of crystalline solids played a prominent role in the early stages of the development of condensed matter physics (Solid State and Statistical Mechanics) [CL95, AM76]. However, alterations of this "perfect" order are ubiquitous in nature. For many practical applications we use materials that are weakly or strongly disordered. An outstanding example are doped semiconductors needed to construct microelectronic devices. Weak disorder is present in many solids through defects, vacancies or dislocations of the crystalline lattice. We say that disorder is strong when long-range order and translational periodicity break down, even though local order might be preserved. This is the case of amorphous solids such as glasses, which do not show any kind of long-range order. Disorder can be realised in many ways other than structural, such as magnetic, orientational (in dipolar materials), chemical and vibrational. For this reason, the physics of disorder is interesting from the point of view of fundamental physics.

Disordered systems display an immense variety of complex static and dynamic phenomena. One of the most interesting, though poorly understood, are those in which the strong randomness induces the frustration of the ground state and, as a consequence, a large degeneracy of the lowest-lying states. The canonical example of disordered systems is the spin glass. The spin glass is the magnetic analogous of a glass. A glass is an amorphous system that exhibits a dynamical transition from a liquid to a metastable solid-like phase in which the dynamics is extremely slow. In spin glasses, this freezing transition is identified with a real thermodynamic transition from a paramagnetic phase to an "ordered" phase called spin glass.

Even though a spin glass is a useless piece of material from the technological point of view, it contains a great deal of fascinating physics. In fact, the study of spin glasses is interesting for fundamental physics not only because they are disordered systems but

also because the simplicity of its modelling makes spin glasses the paradigm of complex disordered systems. Therefore its study can be useful to understand the behaviour of other more complex disordered systems such as gels, polymers or ceramic superconductors [You98]. In this respect it is useful to introduce the notion of complexity. In computer science a complex problem is a problem that cannot be solved in a time that grows polynomially with the number of variables [Pap94]. The notion of complex system has been extended to other fields and gathers a wide range of systems, going from solids to living organisms and social collectivities [Par02]. For its potential applicability the study of complex systems has attired much attention in the last years, especially of statistical physicists, who have tried to understand complex behaviour by reducing the description to a few relevant variables.

Historically experimentalists and theoreticians working on spin glasses have been worried about different problems. Even though from the very beginning it was clear that spin glasses are essentially off-equilibrium systems with very large equilibration times at low temperatures, theoreticians spent a lot of time trying to understand the equilibrium properties of mean-field models. Actually, regardless of whether it is relevant to understand the behaviour of real systems or not, the theoretical treatment of the problem has required the development of new analytical (e.g. Replica and dynamical formalisms [FH91a]), as well as numerical techniques (Parallel and Grand Canonical Tempering and generic Optimisation techniques [MPRL98b]). These advances have given rise to a new phenomenology which goes under the name of glassy phenomena from which different fields have much profited such as neural networks, computer science and disordered electronic systems.

This thesis is an effort to understand some aspects linked to this phenomenology. The primary goal is that of emphasising the importance of large-scale excitations in these systems, an aspect whose complete understanding can provide us with the final solution to one among the most controversial fields in modern Statistical Physics.

Chapter 1

INTRODUCTION TO SPIN GLASSES

A spin glass is a magnetic material with random competing interactions between magnetic moments. As a consequence, the ground state configuration cannot satisfy all the bonds, and thus is *frustrated*. The frustration is at the origin of the complex structure of the free-energy landscape, with many low-energy metastable states that lead to the very slow relaxation toward the equilibrium state as observed experimentally. This slow dynamics, also called *glassy dynamics*, gives rise to a very rich phenomenology with dynamical origin such as ageing, violation of the fluctuation-dissipation theorem as well as the *chaotic features* such as rejuvenation and memory in the magnetic relaxation [VHO$^+$96]. Actually, many of these phenomena are not exclusive of spin glasses, but exhibit striking similarities with other very different glassy systems such as structural glasses, granular systems and pinned defects. This is in general attributed to the universality in the organisation of valleys, saddles and barriers in the complex free-energy landscape.

At high temperatures the system is in a paramagnetic phase. Magnetic moments flip randomly with time, thus the local magnetisation vanishes: $m_i = \langle S_i \rangle = 0$. At low temperatures, however, NMR and neutron scattering measurements reveal that spins *freeze* in random orientations. Therefore, even though the local magnetisation is finite, $m_i \neq 0$, the global magnetisation vanishes, $m = \frac{1}{V}\sum_i m_i = 0$, so that it is not a good order parameter [1]. In this kind of systems we expect that randomness reduces correlations to a few spins. Nevertheless there are very long temporal correlations due to the freezing of the spins. A measure of the local squared magnetisation is given by the average of the auto-correlation function. This is the order parameter proposed by Edwards and Anderson [EA75],

$$q_{\rm EA} = \lim_{t\to\infty} \lim_{V\to\infty} [\langle S_i(t_0) S_i(t_0+t)\rangle] \tag{1.1}$$

[1] The order parameter for anti-ferromagnets, the staggered magnetisation $m_k = \frac{1}{V}\sum_i m_i e^{-i\mathbf{k}\cdot\mathbf{r_i}}$, also vanishes.

where V is the total number of magnetic moments in the system and $[\cdots]$ and $\langle\cdots\rangle$ stand for the averages over all the magnetic moments of the system and over all the possible t_0. This parameter measures if there exist different phases in which the system can get trapped: if the system is ergodic $q_{\rm EA}$ vanishes and remains finite otherwise. At high temperature the system is in a paramagnetic phase so that all the configurations in phase space are explored and $q_{\rm EA} = 0$. Below the freezing temperature ergodicity is broken, so that $q_{\rm EA}$ becomes positive and grows on lowering the temperature until it reaches the zero temperature value $q_{\rm EA}(T = 0)$. Note that in (1.1) the order of the limits is very important: in a finite system the whole phase space is sampled in an finite amount of time so that correlations vanish in the limit $t \to \infty$ even if ergodicity is broken in the thermodynamic limit. Thus, to detect ergodicity breaking one has to take first the limit $V \to \infty$.

The transition into the spin-glass phase is thus a freezing transition in which time-reversal symmetry (TRS) is spontaneously broken as in ferromagnets. This transition is of second order in the thermodynamic sense: the first derivatives of the thermodynamic potentials are continuous, so that there is no latent heat; it is continuous in the order parameter; and relaxation times diverge as the system approaches the critical temperature (critical slowing down). Still, this transition is peculiar because there is not a divergence in the linear susceptibility nor in the specific heat.

In what follows we shall comment on these two aspects and focus on the points which are most closely linked to the subject of this thesis: the thermal properties and the time-dependent dynamical effects in magnetic measurements.

1. Experimental facts

The first experimental evidence of spin glass behaviour was reported in 1972 when Cannella and Mydosh [CM72] found a very pronounced peak in the a.c. susceptibility for very low fields of dilutions of transition elements in noble metal hosts (see Fig. 1.1). The position of the cusp determines the freezing temperature T_f into the SG phase. This freezing temperature was found to depend on the frequency of the a.c. field $T_f(\omega)$ with an extrapolated value for very short frequencies different from zero. This finding implies that there is a transition at a finite temperature $T_f(0)$, but that at very low temperatures the system cannot reach equilibrium within the experimental window. Actually, one of the most distinctive features of spin glasses is that they show effects over a very large time window that spans more than 16 orders of magnitude, from timescales (or inverse frequencies) of $10^{-12}s$ typical of neutron scattering experiments to $10^{4}s$ typical of magnetisation measurements.

1.1 The specific heat

The specific heat contains all the information about the degrees of freedom of the system. Therefore, information about excitations can be extracted from the analysis of the specific heat around the critical temperature and at low temperatures.

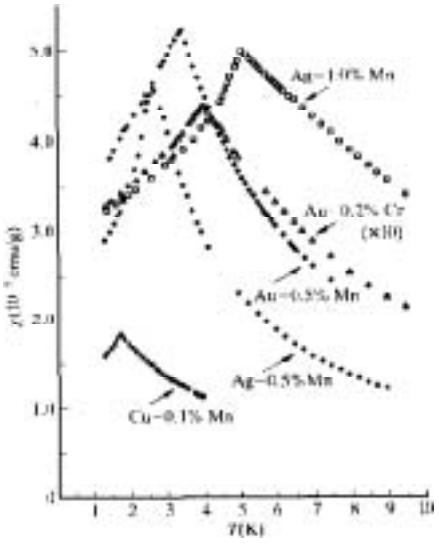

Figure 1.1. Peak in temperature of the a.c. susceptibility at a frequency of 0.01 Hz for different spin glass materials after Cannella and Mydosh [CM72].

At the transition, the specific heat does not diverge, it only shows a broad maximum at a temperature slightly higher than T_f (see Fig. 1.2). This is due to the nature of the transition which goes from a disordered paramagnetic phase to a *less* disordered one, the spin glass phase. The magnetic moments do not freeze suddenly at T_f: spins start freezing at a higher temperature and follow a gradual process until freezing completely at $T = 0$. For this reason, the specific entropy (s) does not have an abrupt change at T_f but decreases rather smoothly with temperature, hence the specific heat is a continuous function of temperature.

At low temperatures, the specific heat vanishes linearly in T. This is a common feature to other systems such as amorphous materials or structural glasses. Following Anderson *et al.* [AHV72] this behaviour can be accounted for if we model the system at low temperatures as an ensemble of two-level systems with an energy barrier. Each two-level system is characterised by its energy gap, Δ [2]. Hence, the partition function at temperature $T = 1/\beta$ reads, $\mathcal{Z} = 1 + e^{-\beta\Delta}$.

[2]One could also extend the argument to a general system where tunnelling processes happen with finite probability at low temperatures, but this would not change the final result.

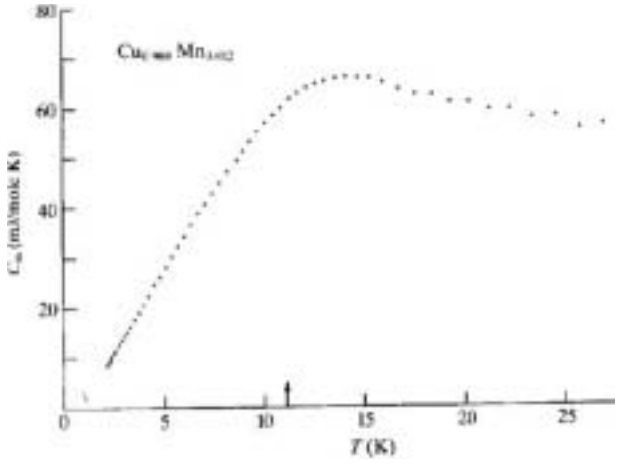

Figure 1.2. Specific heat versus temperature of a spin-glass sample of a dilution of Mn in a Cu matrix. The arrow signals T_f, the temperature at which the peak in the a.c. susceptibility is observed for the same material (from [WK75]).

The specific heat of each subsystem can be obtained from the fluctuation-dissipation relation, $c(\Delta) = \beta^2 \left(\langle E^2 \rangle - \langle E \rangle^2 \right)$ reading,

$$c(\Delta) = \beta^2 \left(\frac{\Delta^2 e^{-\beta\Delta}}{\left(1 + e^{-\beta\Delta}\right)^2} \right) \quad . \tag{1.2}$$

The energy gaps of the whole ensemble are random variables distributed according to the density $\rho(\Delta)$. Therefore, the average specific heat in terms of the variable $x = \beta\Delta$ is expressed as follows,

$$c(T) \;\; = \;\; T \int_0^\infty dx \; \rho\left(T\,x\right) c(\Delta) \stackrel{T \to 0}{\sim} T \; \rho(0) \quad . \tag{1.3}$$

At low temperature $c(T)$ is linear provided the weight of having zero gap is finite, $\rho(0) > 0$. Certainly, this is a very simplified model, but the important point to keep in mind is that there must exist a spectrum of gap-less excitations to have a linear in T behaviour.

1.2 Susceptibility

The linear (static) susceptibility $\chi = \left. \frac{\partial M}{\partial h} \right|_{h=0}$ does not diverge at T_f but shows a rounded cusp. The susceptibility is related to the correlation functions by the fluctuation-dissipation relation,

$$\chi = \frac{1}{V} \sum_{ij} \chi_{ij} \; , \qquad \chi_{ij} = \frac{\langle S_i S_j \rangle - \langle S_i \rangle \langle S_j \rangle}{T} \quad . \tag{1.4}$$

In the high temperature phase it follows a Curie-Weiss law typical of paramagnets $\chi = 1/T$. Below T_f it starts decreasing due to the freezing of the magnetic moments. At low temperatures, the contribution essentially comes from the auto-correlations, χ_{ij}, which are related to the local magnetisations m_i as follows,

$$\chi \sim V\chi_{ii} = \frac{1-m_i^2}{T}\,; \qquad \langle S_i\rangle = m_i\,. \tag{1.5}$$

Since there is no long-range order, the linear susceptibility cannot diverge. Instead, the relevant order parameter $\langle S_i\rangle^2$ acquires long range order and the squared susceptibility diverges at the transition. Thus, it is useful to define the spin-glass susceptibility as,

$$\chi_{\rm SG} = \frac{1}{N}\sum_{ij}\langle S_iS_j\rangle^2 \quad , \tag{1.6}$$

that diverges at T_f and can be characterised with the usual critical exponents. Furthermore, it is related to the non-linear susceptibility $\chi_{\rm nl}$, an observable that can be measured experimentally because it is related to the magnetisation [Cha77],

$$M = \chi\, h - \chi_{\rm nl}h^3 + \cdots\ ; \qquad \chi_{\rm nl} = \beta\left(\chi_{\rm SG} - \frac{2}{3}\beta^2\right) \quad . \tag{1.7}$$

At low temperatures, the linear susceptibility depends strongly on the way the experiment is performed, as expected in an off-equilibrium situation. One of the first phenomena to be observed were the differences between the field-cooled (FC) and zero field cooled (ZFC) susceptibilities (see Fig. 1.3). The experimental protocol is the following: FC: the sample is cooled from above T_f down to low temperature in a small applied magnetic field; ZFC: the sample is cooled with no magnetic field and then a small magnetic field is applied to measure $\chi_{\rm ZFC}$. After the FC process, the signal for $\chi_{\rm FC}$ is stronger than $\chi_{\rm ZFC}$ and, moreover, reversible to a very good approximation, since one can go back and forth in temperature and measure the same magnetisation. In contrast, $\chi_{\rm ZFC}$ displays a sudden irreversible jump when the field is applied and then shows a slow increase until it merges with the curve corresponding to $\chi_{\rm FC}$ in the region above T_f. This relaxation can be extremely slow, a fact that is linked to the existence of many deep valleys in which the system can get trapped depending on the cooling process. At low temperatures, relaxation times become so large that only a part of phase space can be explored during the experimental time window and, thus, leads to irreversibility. This situation is called *weak ergodicity breaking* in literature, because in a finite system ergodicity is effectively broken at finite times.

Irreversibility also manifests in the magnetisation measures, specifically in the differences observed between the thermo-remanent magnetisation (TRM) and the isothermal magnetisation (IRM) for not very small magnetic fields. The TRM is the magnetisation measured when after having cooled the sample in a field, we switch off the field. The

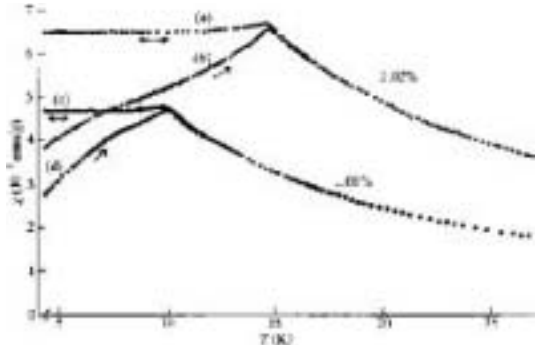

Figure 1.3. ZFC (b & d) and FC (a & c) susceptibilities versus temperature of **Cu**Mn for MN concentrations of 1.08 and 2.02 % after [NKH79]. Curves have been obtained following the protocols described in the text at a magnetic field of $H < 0.05$ Oe. Note that at low temperatures both curves are very different and that only in the region above T_f curves corresponding to both procedures are equivalent.

IRM is the magnetisation measured when after a ZFC protocol a magnetic field is applied during a macroscopic time. This difference disappears with strong applied fields because the SG state is erased.

1.3 Ageing

1.3.1 Isothermal ageing

Ageing refers to the dependence of the dynamical evolution of a system upon its previous history. In spin glasses, it was first observed by Lundgren *et al.* [LSNB83] in the relaxation of the ZFC magnetisation. The procedure is the following: cool the sample from the paramagnetic phase to the non-stationary region. After a certain waiting time (t_w) apply a magnetic field and then measure the growth of the magnetisation during the observation time (t). The total time elapsed from the beginning of the experiment $t_a = t + t_w$ is the *age* of the system. The relaxation was found to depend on both t_w and t in such a way that for a fixed t, the longer the waiting time the slower the response, as if the system had reached a deeper metastable sate (see Fig. 1.4). As long as the applied fields are small, the magnetisation is linear with the field so that the behaviour of the susceptibilities is the same as that observed for the magnetisations (this is the linear response regime). Nevertheless, for high fields the ageing process is affected so differences between both types of measurements are observed [PNS86].

Since the first observations of ageing in amorphous polymers and structural glasses [Str78], ageing has been observed in many other disordered and non-disordered materials presenting a slow evolution toward equilibrium such as orientational glasses, supercooled liquids, gels, foams, granular systems and vortices in superconductors [HVD$^+$00]. The general procedure is the same as before: quench from high temperature to a temperature below T_f (typically the temperature at which the system does not equilibrate within the

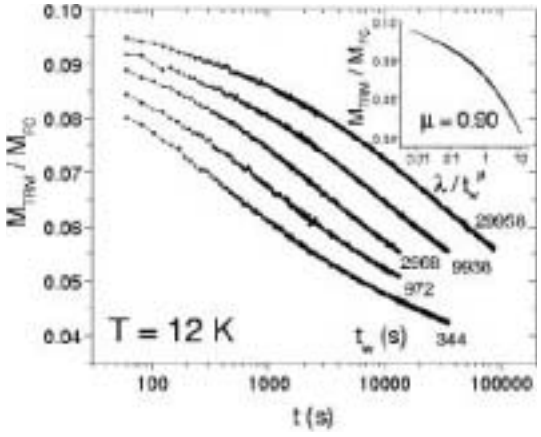

Figure 1.4. Decay of the thermo-remanent magnetisation of the **Ag**Mn 2.6% spin glass for different $t_w = 300,\ 1000,\ 3000,\ 10000$ and $30000\ s$ obtained in [OAH85]. The magnetisation is normalised by the FC value measured just before removing the field ($H = 0.1$ Oe). In the inset the ageing part of the TRM is plotted against the adequate scaling variable as discussed inthe text (for details see [VHO$^+$96]).

experimental time window), wait during t_w and apply a perturbation. This perturbation can be of any nature: a mechanical stress if it is a polymer or an electric field in gels. There is ageing if the measured relaxation curve depends on the waiting time (see Fig. 1.4). Actually, the response to any perturbation can be split into two different contributions [CK93, CK95]: *i)* a stationary part that depends only on $t_{\rm obs}$ and thus is time-translational invariant; and *ii)* an ageing part depending on both times. Hence, we can express the magnetic susceptibility as follows,

$$\chi(t_{\rm obs}, t_w) = \chi_{\rm st}(t) + \chi_{\rm AG}(t_w, t_a)\,; \qquad t_a = t + t_w\ . \tag{1.8}$$

In a.c. measurements it is usual to analyse the out-of-phase component of the susceptibility χ'' because its signal is stronger than that of the in-phase component χ'. In these protocols, the observation time corresponds to the inverse of the frequency of the oscillating magnetic field: $t = 1/\omega$. Because frequencies lower than 0.001 Hz cannot be reached in magnetic measurements the observation window is limited and thus only the very early stages of the ageing process where $\omega t_a \gg 1$ can be investigated. One finds that the shape of the imaginary part of the susceptibility can be parametrised as follows,

$$\chi'' = \chi''_{\rm st}(\omega) + \chi''_{\rm AG}(\omega t_a)\,; \qquad \chi_{\rm AG}(\omega t_a) \sim 1/\left(\omega t_a\right)^b\ . \tag{1.9}$$

The stationary contribution does not depend on age and vanishes, either as ω^a with a small, or as $\ln \omega$. And, the ageing part is a scaling function of the variable ωt_a that vanishes as a power law with an exponent $b > 0$ (see Fig. 1.5).

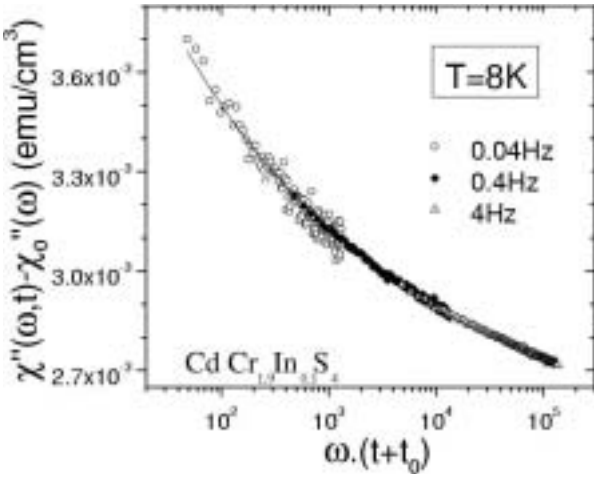

Figure 1.5. Scaling of the χ''-relaxation curves of a sample of $CdCr_{1.9}In_{0.1}S_4$ at $T = 8K$ ($T_f \approx 20K$) for different frequencies $\omega = 0.04,\ 0.4$ and $4Hz$ obtained from [VDA$^+$00]. The curves have been shifted vertically in order to compensate for different equilibrium values, and an off-set time t_0 has been added to account for the fact that the cooling procedure is not instantaneous. The solid line corresponds to a trial fit proposed in [BCKM98]: $\chi''(\omega,t) = \chi''_{eq}(\omega) + [\omega(t+t_0)]^{-b}$, with $b = 0.2$ for both temperatures.

In general, the ageing part of any response is a scaling function with a general scaling variable (see inset Fig. 1.4) [VHO$^+$96],

$$x = \frac{h\left[(t+t_w)/\tau\right]}{h[t_w/\tau]}, \tag{1.10}$$

with τ being a microscopic time. This scaling function can be very different depending on the system. The ωt_a scaling found for the ageing part of the out-of-phase susceptibility is equivalent to the t/t_w obtained in the magnetisation or correlation functions and means that the relaxation time increases proportionally to the age. This scaling is referred to as *full ageing* and is valid for the initial stages of the ageing process when $t(\ll t_w)$ is short. However, for the larger observation times which can be reached in dc measurements, the full ageing scaling overestimates the real ageing process in many cases, a phenomenon known as *sub-ageing* [VHO$^+$ 96]. The relaxation time grows more slowly than age, so that the effective timescale associated with the age t is $\lambda \sim t_w^\mu$ with $\mu < 1$. By appropriately choosing the effective time λ and μ one can scale all the curves with the scaling variable λ/t_w^μ (see inset in fig 1.4).

Another common feature to all glassy systems is that the usual fluctuation-dissipation theorem (FDT) that relates auto-correlation and response functions through temperature $R = -\dot{C}/T$, does not hold for the ageing part because ageing is an out-of-equilibrium phenomenon. This can be better visualised in the so-called FDT plots in which the correlations (magnetisation M) are plotted against the integrated response function (or

susceptibility χ) and the resulting curve is found to substantially deviate from a straight line of slope $-1/T$ [HO02].

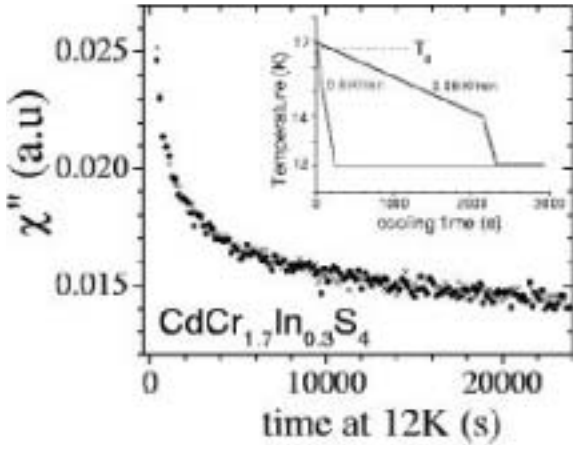

Figure 1.6. Absence of cooling rate effects in the out-of-phase component of the a.c. susceptibility obtained from [VHO$^+$96]. We plot χ'' versus ω for the two different cooling processes shown in the inset. Note that both curves superimpose.

In spite of this common phenomenology, there is a very striking phenomenon observed in spin glasses: *the absence of cooling rate effects in the ageing process*. The relaxation curve measured at temperature $T < T_f$ does not depend on how fast the sample is cooled in the vicinity of the freezing temperature. Only the very late stages at temperatures close to the final temperature affect the final relaxation signal (see Fig. 1.6). This is clearly not the case of systems such as disordered ferromagnets, where the evolution of domain walls at $T < T_f$ is activated over energy barriers. In the latter, relaxations are cumulative so that the previous cooling history amounts to a larger effective waiting time [HVD$^+$00]. The conclusion that can be drawn from this finding is that, in spin glasses, ageing at temperature T_1 does not bring the system closer to its equilibrium state at a lower temperature T_2.

1.3.2 Temperature shift experiments

Recently more sophisticated protocols with magnetic perturbations applied at different stages of the ageing process and temperature shifts have been proposed [RVHO87, GSN$^+$88]. From these experiments *new* dynamical effects have been observed in the out-of-phase susceptibility which are closely related to the disentanglement of the ageing process at different temperatures. These are the *rejuvenation* and *memory* effects to which much attention has been devoted [VHO$^+$96, YLB01, BDHV01, BB02][3]. The

[3]The same effects have been observed in thermo-remanent measurements.

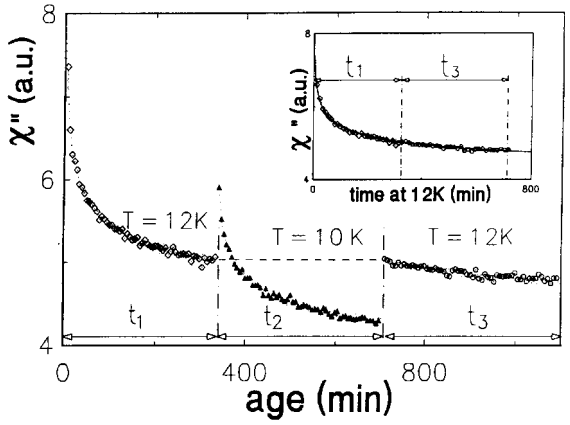

Figure 1.7. Effect of a negative temperature shift $12K \rightarrow 10K \rightarrow 12K$ in the time dependence of χ'' in a sample of $CdCr_{1.7}In_{0.3}S_{0.4}$ ($T_f = 16.7$) at frequency 0.01 Hz obtained after [RVHO87]. The inset shows the relaxation measured during the time spent at $12K$ together with the reference curve obtained for relaxation at $12K$ with no temperature shift.

protocol is the following: quench the sample from the paramagnetic phase down to a temperature T_1 below T_f. Then measure the response to an alternate field of frequency ω, $\chi_{ac}(\omega)$, during t_w. Afterwards, change the temperature by an amount ΔT, and measure the response at $T_2 = T_1 + \Delta T$ during t_w. Then, the temperature is set back to the initial one T_1. If ΔT is negative (see Fig. 1.7), one observes that after changing the temperature the relaxation process starts abruptly from a higher value. The relaxation process does not slow down, but restarts again regardless of the thermal energy reduction. This chaotic-like effect is called *rejuvenation*. Moreover, when heated back to T_1 the relaxation continues exactly from the point where it left it before cooling the sample down to T_2. This is the so-called *memory effect* (see the inset in Fig. 1.7) . These effects are not found in positive shifts of temperature. In this case one observes successive rejuvenation processes upon temperature changes. Therefore, it seems that whereas ageing at low temperatures does not affect ageing at higher temperatures, ageing at higher temperatures is able to erase all the memory of the previous thermal history. Of course, these effects take place provided the temperature difference is sufficiently large since otherwise ageing at different temperatures becomes cumulative. This has been interpreted in terms of hierarchical dynamics: each level of description or length scale has its own independent dynamics. To each temperature one can associate the length scale explored at t_w so that if length scales at different temperatures are sufficiently separated, the ageing processes at different temperatures are independent [FH88b, BDHV01].

These effects can be better visualised in the temperature cycling protocols [DJN99] (see Fig. 1.8), in which the χ'' is measured as a continuous function of temperature at constant cooling rate. In a second run the same procedure is followed but several stops

are made at a reference temperature, $T^* < T_f$, and the system is let to age during t_w . Then the cooling down is resumed. On heating back, one can observe that χ'' shows a big dip close to T^* and, exactly at T^*, χ matches the values reached at the end of the ageing process (see Fig. 1.8). Thus, the memory of the ageing process has been kept in the system during all the cooling protocol. All these memory and rejuvenation phenomena have been recently observed in other materials such as disordered ferromagnets, dipolar glasses, polymer glasses (PMMA) or gelatin [HVD$^+$00, JVH$^+$98, VHO$^+$96].

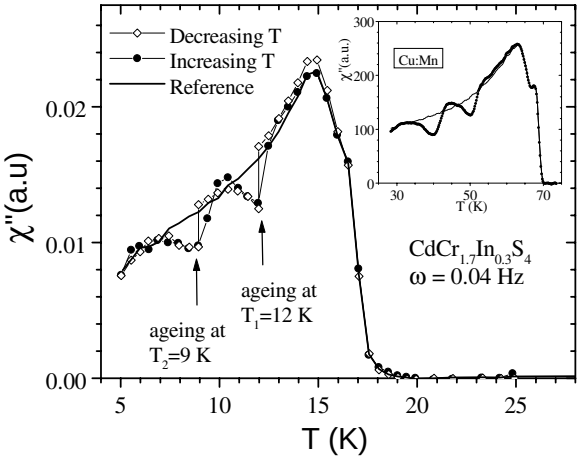

Figure 1.8. Temperature cycling experiment in the χ'' of the $CdCr_{1.7}In_{0.3}S_{0.4}$ from [JVH$^+$98]. While cooling down at a constant rate two stops have been made at $12K$ and $9K$ during $7h$ and 40 min respectively. The solid line corresponds to continuous reheating after continuous cooling. In the inset the same experiment is shown for the **Cu**Mn spin glass from [DJN99]

We have to stress, though, that the recovery of memory is not always perfect. If ΔT is too small, the stay at T_2 affects the ageing at T_1 so that an effective time (smaller than t_w) has to be added to take into account the time spent at T_2. Moreover, for short times after the heating process, there is sometimes a small transient known as *memory anomaly* [SVDV02]. This anomaly is a non-monotonous function of ΔT. For small ΔT the reference curve is reached from below whereas for larger ΔT perfect memory is reached from above.

1.4 Materials

Since the early seventies when this *new* magnetic behaviour was found in diluted gold-iron alloys, more and more different classes of spin-glass materials have emerged [BY86, Myd93]. These can be classified according to the nature of the magnetic interaction.

The first spin-glass materials studied belong to the RKKY category (for Ruderman and Kittel [RK54], Kasuya [Kas56] and Yosida [Yos57]) named after the particular interaction at the origin of the spin glass behaviour. In these materials the magnetic interaction is due

to the scattering of the conduction electrons surrounding the magnetic moments, which leads to an indirect exchange interaction which oscillates strongly with the distance to the magnetic moment [AM76],

$$J(r) = J_0 \frac{\cos\left(2\kappa_{\rm F} r\phi\right)}{\left(\kappa_{\rm F} r\right)^3} \quad , \tag{1.11}$$

where $\kappa_{\rm F}$ is the Fermi wave vector of the host metal and J_0 and ϕ are constants. The randomness in such systems is realised by the random position of the magnetic impurities which leads to alternate sign of spin-spin interactions. This class includes crystalline metallic solids such as Au, Ag, Cu or Pt with sufficiently diluted magnetic impurities such as Fe or Mn, but also alloys with rare earth components (e.g. YDy or ScTb) as well some ternary systems (e.g. $La_{1-x}Gd_xAl_2$).

Another class are insulating spin glasses such as $Eu_xSr_{1-x}S$ in which the Eu is substituted by the non-magnetic Sr. The same features are found in other materials where Mn is the magnetic constituent and the role of S is played by Cd, Cr or Z. In this alloy the competition of interactions appears because nearest-neighbours are coupled ferromagnetically whereas next-nearest-neighbours are coupled anti-ferromagnetically. It is interesting to note that for low Eu concentrations the system never develops magnetic order at low temperature whereas for large x the system orders ferromagnetically. Thereby, this kind of materials can also display transitions changing x and also exhibit *reentrant phases* in the $T - x$ phase diagram [BY86]. This means that for fixed x the material can undergo a transition from a SG phase to a FM phase at lower temperatures. This effect is also present in RKKY spin glasses for high enough concentrations of magnetic impurities.

Another class of spin glasses are amorphous materials compounded by rare earth and transition metals such as Fe_xNi_{1-x} or La_xGd_{1-x}. However the microscopic origin of the interaction is difficult to determine. Besides, one can also find spin glass behaviour in magnetic insulators and even in systems with no magnetic component such as ferroelectric-anti-ferroelectric mixtures (e.g. RbH_2PO_4 and $NH_4H_3PO_4$) in which the role of the spin is played by the dipolar moment or molecular glasses (e.g. mixtures of para- and ortho- hydrogen) in which the orientation of the electric quadrupole moment is frozen at low temperatures.

2. Theoretical facts

The theoretical activity in the field began in 1975 when Edwards and Anderson [EA75] formulated a model that, leaving aside the microscopic details of the real system, captured the essential physics of a spin glass. In this model the magnetic moments S_i are taken to be Ising variables sitting on a cubic lattice. Previously, we have described the RKKY interaction that leads to SG behaviour in some materials. Even though this interaction is absolutely isotropic, in these systems there is anisotropy coming from dipolar and

Dzyaloshinski-Moriya type interactions so that many spin glass materials are effectively of the Ising type [4].

The so-called EA model is defined by the following Hamiltonian,

$$\mathcal{H} = -\sum_{\langle i,j \rangle} J_{ij} S_i S_j - h \sum_i S_i \quad . \tag{1.12}$$

where sums are usually restricted to nearest neighbours and h is the external magnetic field. Couplings are independent random variables drawn from a probability distribution $P(J_{ij})$ which in most of the cases is either Gaussian with zero mean and variance σ ,

$$P(J_{ij}) = \frac{1}{\sqrt{2\pi\sigma^2}}\, e^{-\frac{J_{ij}^2}{2\sigma^2}} \quad , \tag{1.13}$$

or bimodal (also referred to as $\pm J$) with two possible values J and $-J$,

$$P(J_{ij}) = \frac{1}{2}\,\delta(J_{ij} - J) + \frac{1}{2}\,\delta(J_{ij} + J) \ . \tag{1.14}$$

Note that in this model, the randomness is realised through the couplings between the magnetic moments (J_{ij}) and not through the positions, nevertheless, these two types of randomness are supposed to yield similar results [BY86].

2.1 Basic concepts

Spin glass models are characterised by the frustration present in the magnetic configurations due to the existence competing random interactions between spins. There are two types of variables: *annealed* and *quenched*. The former correspond to the magnetic moments or spins that change with time and temperature, and the latter to the couplings that are fixed at all temperatures.

- Averages
  As usual in Statistical Mechanics the important thermodynamical potential at fixed temperature T and volume (the number of spins) V is the Helmholtz free-energy,

  $$F = E - k_{\rm B}\, T\, S\,; \qquad F = -T k_{\rm B}\, \ln \mathcal{Z} \ . \tag{1.15}$$

  Here, E is the energy, S is the entropy and $k_{\rm B}$ is the Boltzmann constant. For simplicity, in what follows we shall take the convention $k_{\rm B} = 1$.

  In general, a disordered system is defined by the Hamiltonian, $\mathcal{H}(J, \{S\})$, that depends on both types of variables. To obtain the free-energy or any thermodynamical quantity one has two perform an average over the quenched disorder in addition to the standard

[4] Heisenberg type spin glasses also exist, in this kind of systems the transition into the SG glass order is probably due to the onset of chiral order [FH91a].

thermal average in the canonical ensemble. The thermal average at temperature $T = 1/\beta$ is taken at a fixed realisation of the quenched disorder and is denoted by $\langle \cdots \rangle_J$, where hereafter the label J stands for a fixed disorder realisation. Thus, for a given observable $\mathcal{O}$ we have,

$$\langle \mathcal{O} \rangle_J = \sum_{\{S\}} \frac{\mathcal{O}(\{S\})\ e^{-\beta\ \mathcal{H}(\{S\},J)}}{\mathcal{Z}_J}\,; \qquad \mathcal{Z}_J = \sum_{\{S\}} e^{-\beta\ \mathcal{H}(\{S\},J)}\ . \tag{1.16}$$

Where $\mathcal{Z}_J$ is the partition function. The average over all possible realisations of the disorder is given by,

$$\overline{\langle \mathcal{O} \rangle_J} = \int \prod_{ij} dJ_{ij}\ P(J_{ij}) \langle \mathcal{O} \rangle_J \tag{1.17}$$

where $\overline{(\cdots)}$ denotes the average over all possible samples. Therefore, the average free-energy reads, $F = \overline{F_J} = -k_{\rm B}\ T \overline{\ln \mathcal{Z}_J}$.

Note that real materials correspond to a single sample of the couplings. Thus, in order to compare theory with experiments, one would like to compute F_J rather than its average, F. Unfortunately, this is impossible because we do not know the microscopic arrangement of all the magnetic moments and their interactions. Nevertheless, as we show in Sec. 2.2.2, the free-energy is a self-averaging quantity which implies that in the thermodynamic limit $F_J = F$. Therefore, the free-energy of a large sample can be obtained from the disorder-averaged free-energy, F.

- Replica Trick

  The computation of the average of the logarithm of $\mathcal{Z}_J$ is usually a hard task. An alternative technique is the Replica Method [EA75, MPV87]. The starting point is the following definition of the logarithm,

  $$\ln x = \lim_{n \to 0} \frac{x^n - 1}{n} \quad . \tag{1.18}$$

  To compute the free-energy one needs to calculate the average over the disorder of $\mathcal{Z}_J^n$, the partition function of n identical and independent systems that we call *replicas*,

  $$\mathcal{Z}_J^n = \sum_{\{S^a\}} e^{-\beta \left[\sum_{a=1}^n \mathcal{H}(\{S^a\})\right]}\ , \tag{1.19}$$

  where a is the replica index.

  The average free-energy is obtained as follows,

  $$\overline{\mathcal{Z}_J^n} = e^{-\beta\ V\ f(n,\mathcal{H})}\,; \qquad f = \frac{F}{V} = \lim_{n \to 0} \frac{f(n,\mathcal{H})}{n} \tag{1.20}$$

  where we have introduced the intensive free-energy, f. Hence if the analytical continuation in the limit $n \to 0$ is possible we can compute the average free-energy from the free-energy of the replicated system.

This method is very useful to perform the average over the disorder. However, one introduces an effective interaction between replicas which complicates the analytical treatment. Besides, it is important to point out that at a practical level the limits $n \to 0$ and $V \to \infty$ are interchanged, because in order to obtain $f(n, \mathcal{H})$ one needs to solve the saddle-point equations obtained in the thermodynamic limit.

- Order Parameter

  We have already introduced the $q_{\rm EA}$ in (1.1), which is the order parameter proposed by Edwards and Anderson that measures the freezing of the spins. When dealing with replicas the relevant order parameter is the *overlap* that corresponds to the scalar product between two copies of the system (a, b),

$$q_{ab} = \frac{1}{V}\sum_{i=1}^{V} S_i^a \, S_i^b \,, \qquad q = \frac{2}{n(n-1)} \sum_{1 \le a < b \le n} \overline{\langle q_{ab} \rangle} \tag{1.21}$$

  Note that the overlap can take any value in the range $[-1, 1]$. In mean-field theory, the equilibrium order parameter, q, is not equal to $q_{\rm EA}$. This difference arises because apart from the two regions corresponding to positive and negative overlap which appear due to the breaking of TRS in the thermodynamic limit, phase space is further split in several ergodic components. This means that there are different *pure states*, that we will label α, which have no connected correlations in the limit $V \to \infty$ [MPV87]. The $q_{\rm EA}$ defined in (1.1) corresponds to the average self-overlap of each pure state and measures the average value of the squared local magnetisation in a single valley or ergodic phase [MPV87],

$$q_{\rm EA} = \frac{1}{V}\sum_i \langle S_i \rangle_\alpha^2 = \frac{1}{V}\sum_i \left(m_i^\alpha\right)^2 \quad , \tag{1.22}$$

  where $\langle \cdots \rangle_\alpha$ denotes the thermal average restricted to those configurations belonging to the same pure state α. Therefore, $q_{\rm EA}$ is the maximum value that q can take. Furthermore, overlaps between different states do not vanish. As pointed out by Parisi [Par83], the adequate order parameter that reflects this scenario is the probability distribution of the overlap, $P(q) = \overline{P_J(q)}$, that for a single sample reads,

$$P_J(q) = \frac{2}{n(n-1)} \sum_{1 \le a < b \le n} \langle \delta \left(q - q_{ab}\right) \rangle_J \quad . \tag{1.23}$$

  A particularity of the $P(q)$ is that, in contrast to F, it exhibits finite sample-to-sample fluctuations even in the thermodynamic limit and thus it is not self-averaging (see Sec. 2.2.2).

2.2 Mean-field theory: the Sherrington-Kirkpatrick model

One of the main achievements in the field is the solution of the mean-field theory found by Parisi [Par79]. The understanding of such a theory introduced a lot of new

concepts: the definition of a proper order parameter $P(q)$, ultrametricity and the breaking of ergodicity which gave rise to the well known picture of a free-energy landscape with a hierarchical structure of wells within wells.

In what follows we will focus on the Sherrington-Kirkpatrick model (SK), but we note that the general framework is valid for any mean-field model. The SK model is the mean-field version of the EA model (1.12) in which all spins interact with each other. It is defined by the following Hamiltonian,

$$\mathcal{H} = -\sum_{i<j} J_{ij}\ S_i S_j\ -\ h\sum_i S_i\,; \qquad S_i \pm 1\quad . \tag{1.24}$$

The variance of the distribution of the couplings has to be chosen in order that the energy is extensive, so that for Gaussian couplings the distribution reads,

$$P(J_{ij}) = \frac{1}{\sqrt{2\ \pi\ \sigma^2}} e^{-\frac{J_{ij}^2}{2\ \sigma^2}}\,; \qquad \sigma^2 = \frac{J^2}{V}\quad . \tag{1.25}$$

For simplicity, $J^2 = 1$ in what follows.

In order to solve this model one must use the replica formalism described previously. This method allows to perform the average over the quenched disorder at the cost of introducing a coupling between different replicas. In the SK model the average of the n-replicated partition function can be expressed as [MPV87],

$$\overline{\mathcal{Z}^n} = \int \prod_{a<b} \left[dQ_{ab} \left(\frac{V\beta^2}{2\pi} \right)^{1/2} \right] e^{-V\mathcal{A}[Q]} \tag{1.26}$$

$$\mathcal{A}[Q] = -\frac{n}{4}\beta^2 + \frac{1}{2}\beta^2 \sum_{1\le a<b\le n} Q_{ab}^2 - \ln \mathcal{Z}_1[Q] \tag{1.27}$$

$$\mathcal{Z}_1 = \sum_{\{S\}} e^{\left[-\beta\left(-\beta\sum_{1\le a<b\le n} Q_{ab}^2 S_a S_b - h\sum_a S_a\right)\right]} \tag{1.28}$$

where $\mathcal{Z}_1$ is the partition function of a single site and Q_{ab} is a symmetric squared matrix $(n \times n)$ with zeroes along the diagonal.

The free-energy of the n replicas in equation (1.20) is obtained by solving the saddle-point equations $\frac{\partial A}{\partial Q_{ab}}\Big|_{\min} = 0$ from which we get $\mathcal{A}_{\min}[Q]$ that yields the maximum contribution to the exponential in (1.26). The free-energy of the n-replicated system is immediately obtained as $f(n,\mathcal{H}) = \frac{\mathcal{A}_{\min}[Q]}{\beta}$.

The solution of the saddle-point equations can be expressed in the form of self-consistency equations which read,

$$Q_{ab} = \langle S_a S_b \rangle_{\mathcal{Z}_1} = \overline{\langle S_a S_b \rangle} \tag{1.29}$$

where the thermal average $\langle \cdots \rangle_{\mathcal{Z}_1}$ is evaluated with respect to $\mathcal{Z}_1$ (1.28). Hence the $P(q)$ introduced in (1.23) can be expressed in terms of the Q_{ab}'s as well,

$$P(q) = \lim_{n\to 0} \frac{1}{n(n-1)} \sum_{a<b} \delta(q - Q_{ab}) \quad . \tag{1.30}$$

This last result puts forward that the replica matrix Q_{ab} contains all the information about the low-temperature phase. Moreover, to avoid divergences in the limit $n \to 0$, one must ensure the extensivity of $f\,(n,T)$ in (1.20) by imposing that the sum of all the elements of a row or column of these matrices $\sum_b Q_{ab}$ is independent of the row/column. This is the so-called *replica equivalence* property and its implications go further by establishing a set of identities between the joint distribution of several overlaps (see Sec. 2.1) [Par98].

2.2.1 Breaking replica symmetry

For simplicity let us discuss the case without magnetic field ($h = 0$). The same results are also found in the case in a field that will be discussed more in detail in Sec. 1.1.1.

Usually in pure systems there is permutation symmetry among replicas and thus all the elements in the Q_{ab} matrix are equal. This is the solution that corresponds to the *replica symmetric ansatz* (RS) that holds in the high temperature paramagnetic phase where all the elements in the matrix vanish, $Q_{ab} = q = 0$. On lowering the temperature, it turns out that the stability matrix (or Hessian) , $H = \frac{\partial^2 \mathcal{A}}{\partial Q_{ab} \partial Q_{bc}}$, develops negative eigenvalues so that the symmetric solution becomes unstable. This determines the transition temperature $T_c = 1$. Below this temperature, there is no longer symmetry among replicas and a *replica symmetry broken ansatz* (RSB) has to be proposed. The specific way to break replica symmetry was found by Parisi [Par79].

Thus, at the transition there are two symmetries which are spontaneously broken: *i)* time-reversal symmetry (TRS) (or Z_2 symmetry, as well as in ferromagnets) and *ii)* replica symmetry (RS). The latter means that there are more than two *pure states*, *i.e* states whose connected correlations at long distances vanish (namely the states with magnetisations $\pm m$ which exist in a ferromagnet and that here would correspond to $\pm q_{\rm EA}$). The (euclidean) distance between two pure states (α, β) is related to their overlap,

$$d^2_{\alpha,\beta} = \frac{1}{4\,V} \sum_i \left(S_i^\alpha - S_i^\beta \right)^2 = \frac{1}{2} \left(q_{\rm EA} - q_{\alpha\beta} \right) \tag{1.31}$$

and the distribution of the overlaps is the order parameter (1.23).

The consequences of this broken ergodicity formally expressed as RSB are twofold. First, the organisation of the states is such that they follow the structure of an ultrametric tree. Ultrametricity means that given three replicas $a,\ b$ and c the distances between them are such that,

$$d_{ab} = \max\{d_{ac}, d_{bc}\} \quad . \tag{1.32}$$

Geometrically this means that with the relative distances between a set of three replicas (or states) we can construct triangles which are either equilateral or isosceles with the two equal sizes larger than the other one.

And second, the order parameter has strong sample-to-sample fluctuations in the low-temperature phase. This is equivalent to say that the joint probability of two overlaps does not factorise,

$$P\left(q_1, q_2\right) \neq P(q_1)\ P(q_2) \tag{1.33}$$

Parisi matrices

The simplest way in which one can break replica symmetry is the *one-step RSB ansatz*. In this scheme, the n replicas are divided into m blocks, each containing n/m replicas. The elements of the matrix Q_{ab} can take two different values: q_1 if replicas belong to the same group and q_0 if replicas belong to different groups. The Q_{ab} matrix is constructed with $m \times m$ boxes along the diagonal. The elements inside these boxes are equal to q_1 (we recall that the diagonal terms are equal to zero) and q_0 in the off- diagonal bocks as it is shown below for the case $n = 9,\ m = 3$,

$$\begin{pmatrix}
0 & q_1 & q_1 & q_0 & q_0 & q_0 & q_0 & q_0 & q_0 \\
q_1 & 0 & q_1 & q_0 & q_0 & q_0 & q_0 & q_0 & q_0 \\
q_1 & q_1 & 0 & q_0 & q_0 & q_0 & q_0 & q_0 & q_0 \\
q_0 & q_0 & q_0 & 0 & q_1 & q_1 & q_0 & q_0 & q_0 \\
q_0 & q_0 & q_0 & q_1 & 0 & q_1 & q_0 & q_0 & q_0 \\
q_0 & q_0 & q_0 & q_1 & q_1 & 0 & q_0 & q_0 & q_0 \\
q_0 & q_0 & q_0 & q_0 & q_0 & q_0 & 0 & q_1 & q_1 \\
q_0 & q_0 & q_0 & q_0 & q_0 & q_0 & q_1 & 0 & q_1 \\
q_0 & q_0 & q_0 & q_0 & q_0 & q_0 & q_1 & q_1 & 0
\end{pmatrix} \tag{1.34}$$

From (1.30), within this ansatz the $P(q)$ consists of two peaks at $q = q_1$ and $q = q_0$,

$$\begin{aligned}
P(q) &= \lim_{n\to 0} \frac{1}{n(n-1)} \left[(n-m)\ \delta(q-q_0) + (m-1)\delta(q-q_1)\right] && (1.35)\\
&= m\ \delta(q-q_0) + (1-m)\delta(q-q_1) && (1.36)
\end{aligned}$$

as is shown in Fig. 1.9. Note that for integer n, m is an integer between 1 and n. However, once we have taken the limit $n \to 0$, in order to keep $P(q)$ non-negative, m must become a real number in the range $[0, 1]$.

This is the solution found in a generic class of mean-field models known as p-spin models for $p > 2$ that will be addressed in Sec. 1.1.

The final solution to the SK model is obtained by iterating the previous scheme an infinite number of times. This is the so-called *full-step RSB*. The elements of the matrix become a continuous function $q(x)$ of the parameter $x \in [0, 1]$ that is in turn a function of temperature. x is the equivalent to the size of the blocks m in the one step RSB ansatz and bears the following relation with the order parameter: $dx/dq = P(q)$. The $P(q)$ in the low-temperature thermodynamic phase becomes a non-trivial function of q with support between 0 and $q_{\rm EA}$ (see in Fig. 1.9). Note that q has a plateau at $q_{\rm EA}$ which implies

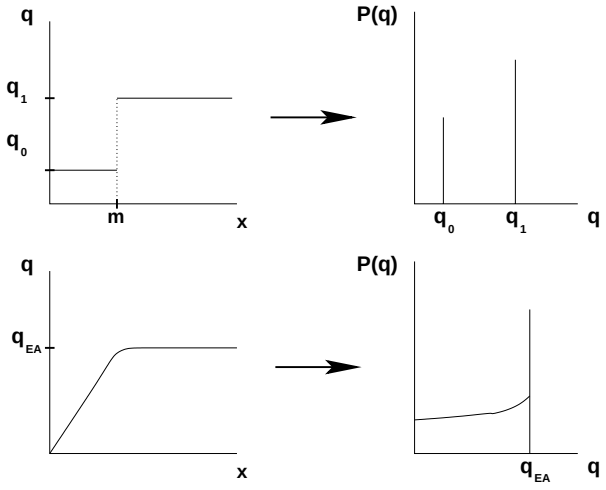

Figure 1.9. q as a function of x and $P(q)$ in the one-step (*top*) and full-step (*bottom*) RSB ansätze.

having a delta peak in the probability distribution at $q = q_{\rm EA}$. For the one step ansatz one can establish the same relation between the elements of the matrix, q_1 and q_0, and the parameter x. In this case q is a discontinuous function of x (see Fig. 1.9): it consists of two plateaus with a breaking point at $x = m$, which leads to the two peak structure of the $P(q)$ (1.36).

Note that this is true only at finite temperature since, at $T = 0$, $q_{\rm EA} = 1$ and the $P(q)$ is trivial: $P(q) = \delta(q-1)$ [5].

We have to point out that the full-step RSB solution recovers the correct thermodynamics because the entropy is always positive. However, the solution is only marginally stable since the spectra of the eigenvalues of the Hessian matrix extends down to zero [DK83], implying that the spin-glass susceptibility diverges in the whole low-temperature phase.

2.2.2 Self-averaging and order parameter fluctuations

One of the central points in the treatment of disordered systems is the *self-averaging* hypothesis. This hypothesis establishes that all the extensive thermodynamic quantities X have sample-to-sample fluctuations of variance $\mathcal{O}(V)$ so that in the thermodynamic limit,

$$\lim_{V\to\infty} \frac{\overline{\mathrm{X}^2} - \overline{\mathrm{X}}^2}{\overline{\mathrm{X}}^2} \sim \frac{1}{V} \to 0 \ . \tag{1.37}$$

[5] Here we are only considering the positive region of q. For systems containing TRS in the Hamiltonian we have that $P(q)$ is symmetric around 0 and, therefore, at $T = 0$: $P(q) = \frac{1}{2}\delta(q+1) + \frac{1}{2}\delta(q-1)$.

Such a statement is crucial in order to compare any theoretical result with experiments, since it means that in the thermodynamic limit averaging over all the set of samples of the quenched disorder yields equivalent results to those obtained from a very large system in which we suppose that all the samples, as subsystems, are realised at a time. This hypothesis is supported by the fact that experimentally one does not observe discrepancies between the measurements of different samples.

Indeed, Brout (1956) proved the validity of such a statement for short-ranged systems using the following very general argument. Consider a very large system of volume V that is divided in N subsystems of volume v, such that $N = V/v$ is large. In the large volume limit, keeping N fixed, we have an equally large number of big subsystems. The free-energy of each subsystem, f_i, is, thus, a random variable whose average is extensive with the size of the subsystem v, $\overline{f_i} \sim v$. The global free-energy is the sum of the free-energies of the N subsystems, $\sum_{i=1,N} f_i \sim N\ v = V$, plus the term accounting for the interactions between subsystems $\sum_{i<j} f_{ij}$. As long as the interactions are short-ranged, the interaction term will be proportional to the surface and thus much smaller than the sum of the free-energies of each subsystem, which scales with the system size. Hence, the global free-energy in the thermodynamic limit is a sum of a large number of random variables. In virtue of the *law of large numbers*, the total free-energy is a normal distributed variable with mean $F \sim V$ and variance $\sim V$.

Therefore, it is clear that the free-energy is SA, and that the same argument is applicable to its derivatives. Nonetheless, this property does not hold for the order parameter because the order parameter distribution cannot be expressed in terms of the derivatives of the averaged free-energy. This is only possible for the $q_{\rm EA}$ which, in the low-temperature phase, is related to the susceptibility as follows (1.5),

$$\chi \sim \frac{1 - \left(m_i^\alpha\right)^2}{T} = \frac{1 - q_{\rm EA}}{T} \quad . \tag{1.38}$$

Which is different from the susceptibility (1.4), $\chi = \frac{1-\int q\, dq}{T}$, due to the breaking of ergodicity at low temperature.

As we have already pointed out, in MFT the order parameter displays very strong sample-to-sample fluctuations in the thermodynamic limit due to the existence of many ergodic phases. What is the situation met in short-ranged spin glasses is still an open question that will be investigated in this thesis.

2.2.3 TAP approach

An alternative approach is the one proposed by Thouless, Anderson and Palmer [TAP77], who derived coupled self-consistent equations for the local magnetisations m_i by making a high temperature expansion. The so-called TAP equations read,

$$m_i = \tanh\left[\beta\left(\sum_{ij} J_{ij} m_i + h_i - \beta \sum_j J_{ij}^2 (1 - m_i^2)\ m_i\right)\right] \quad . \tag{1.39}$$

These are found to have a functional form very similar to those of the local magnetisation obtained in the MFT of ferromagnets except for the Onsager reaction term, $J_{ij}^2(1-m_i^2)$, that describes the contribution to the local field acting on spin S_i coming from spin S_i itself.

Above T_c, the TAP equations in the limit $V \to \infty$ have only one paramagnetic solution with $m_i = 0$. However, below T_c there exist a large number of solutions $\mathcal{N}_s$ that increase exponentially with size V: $\mathcal{N}_s \sim \exp[\alpha(T)\ V]$ where $\alpha(T)$ is a function of temperature that vanishes at T_c [BM80]. The important point is that a large number of them correspond to local minima and saddles with free-energies very close to the ground state. Some of these solutions ($\sim V^\alpha$) are assumed to become in the thermodynamic limit the pure states separated by infinite energy barriers.

This structure of the free-energy landscape provides a very appealing picture to explain experimental results. It is believed, at least at a dynamical level, that a finite-dimensional system is a smeared out version of a MF spin glass. The idea is that there exist many low-energy states that are relevant in dynamical processes, so that the experimental observations at finite times would be the result of probing different local minima of the free-energy landscape.

2.3 Scaling theories: the droplet model

The existence in MFT of an infinite number of ergodic phases is one of the main differences with the phenomenological theory developed for short-ranged spin glasses by Fisher and Huse [FH86], Bray and Moore [BM87] and also Koper and Hilhorst [KH88].

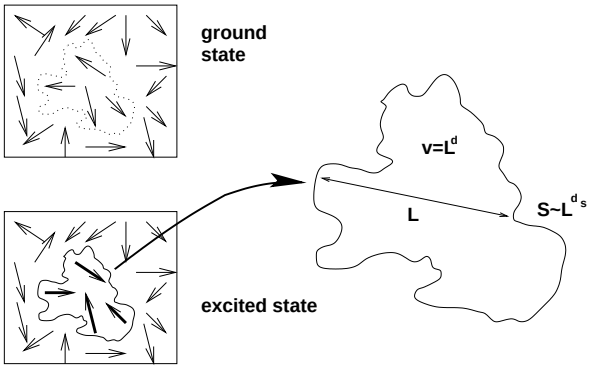

Figure 1.10. Schematic picture of a droplet in 2 dimensions. It consists of a region of spins reversed with respect to the ground state configuration. The droplet is a compact object of linear size L and volume $v \sim L^d$ with a surface of fractal dimension d_s, $S \sim L^{d_s}$, $d-1 < d_s < d$.

The droplet model aims at describing the low-temperature phase of a spin glass using renormalisation group ideas. Within this picture a spin glass is a disguised ferromagnet with only one ground state (and its fully reversed configuration) in which the spins

are frozen in random orientations. Therefore, at equilibrium, the overlap can take two possible values $q = \pm q_{\rm EA}$ and the $P(q)$ is trivial: $P(q) = \frac{1}{2}\delta\left(q - q_{\rm EA}\right) + \frac{1}{2}\delta\left(q + q_{\rm EA}\right)$.

The low-temperature phase is described by the physics close to $T = 0$. Thus, at each temperature well below the critical temperature, a spin glass is described by the ground state plus excitations or droplets of different linear sizes L. As schematised in Fig. 1.10, a droplet is a compact cluster of spins of volume L^d and fractal surface L^{d_s} such that $d - 1 < d_s < d$. The typical free-energy cost to overturn a droplet of size L is $F_L^{typ} \sim \Upsilon(T)\ L^\theta$ where Υ and θ are the stiffness constant and exponent respectively [6]. The free-energy associated to each droplet is broadly distributed, but as there are excitations nearly degenerate with the ground state, the distribution has a finite weight at zero free-energy,

$$\rho(F_L) = \frac{1}{F_L^{typ}}\,; \qquad \tilde{\rho}\left(\frac{F_L}{F_L^{typ}}\right) \qquad \tilde{\rho}(0) > 0 \quad . \tag{1.40}$$

Since the spins at the boundaries have random orientations, it is expected that the energy cost needed to overturn a droplet is smaller than that needed to overturn a ferromagnetic domain wall and thus $\theta < \frac{d-1}{2}$. For this same reason, the spins at the boundaries are extremely sensible to an external a perturbation and in particular against a change in temperature: the equilibrium configurations at two different temperatures are different beyond a crossover length scale $l_{\Delta T}$. This the *chaotic length* associated to chaos in spin glasses [BM87] which has recently been advocated to be responsible for the rejuvenation effects observed experimentally [YLB01] (see Chap. 5).

One of the most controversial predictions of this picture is that the spin glass phase cannot survive in the presence of a magnetic field, in opposition to the results obtained in MFT where there is SG order in a field below the AT line (see Sec. 1.1.1). Simple scaling arguments show that the magnetic field is a relevant perturbation which prevents the system from acquiring spin-glass order even at low temperatures for length scales larger than [FH88a],

$$l_h = \left(\frac{\Upsilon}{h\ q_{\rm EA}}\right)^{\frac{2}{d-2\theta}} \quad . \tag{1.41}$$

Experimental observations point in different directions [MJN$^+$95, PFC99]. Nevertheless, as pointed out by Bray [Bra88], the existence of a relevant perturbation does not necessarily imply that there is no transition in a field.

The thermal exponent θ plays a central role in this theory. Its sign decides whether SG order is stable or not with temperature. On the one hand, if $\theta > 0$ large regions can be flipped with a low energy cost implying that zero temperature order is not stable against thermal fluctuations. When there is a critical point exactly at $T = 0$, the ordered domains survive at a finite temperature up to a length $\xi \sim T^{-1/\theta}$ that diverges exactly at $T = 0$

[6] The linear size of the droplet here is an adimensional length $L = L_{\rm real}/L_0$ where L_0 is a microscopic length scale.

so that θ is related to the correlation length exponent $\nu = -1/\theta$. On the other hand, if $\theta > 0$, large droplets happen with vanishingly small probability in the thermodynamic limit, and, therefore, the zero temperature order is preserved at finite temperature. The marginal case $\theta = 0$ is precisely the case of MFT. Since the $P(q)$ has a finite weight at $q = 0$, there must be large excitations with a cost in free-energy of $\mathcal{O}(1)$. As a matter of fact, in the SK model the free-energies of the different pure states F^α are independent random variables with an exponential distribution: $\rho(F^\alpha) \sim e^{[\beta x(F^\alpha - F_{\rm eq})]}\Theta(F^\alpha - F_{\rm eq})$, where $F_{\rm eq}$ is the equilibrium free-energy and $x(q)$ is the inverse function of the overlap $q(x)$ [MPV85]. Therefore, in order to have a well-defined thermodynamics, only states whose free-energies differ in a constant of $\mathcal{O}(1)$ from $F_{\rm eq}$ will contribute significantly at low temperatures. Hence, we read off $\theta = 0$ because $\rho(F)$ does not explicitly depend on V((1.40)) and, thus, excitations of any size are allowed with finite probability in the infinite-size limit.

Measurements of this exponent have been carried out with different numerical techniques. The most famous one is the domain wall method proposed by McMillan to study excitations in EA spin glasses and finite-dimensional models in general.

2.3.1 The domain wall method

This method is schematised in Fig. 1.11 for a 2d system. It consists in creating a domain wall (DW) across the system as follows: first we compute the ground state energy E of a given sample with periodic boundary conditions (PBC). Then we change from periodic to anti-periodic (APBC) the boundary conditions along one of the directions of the lattice and we compute the energy E' of the new ground state. The configurations of the two ground states will differ in the existence of a DW of broken bonds along the directions perpendicular to the direction in which the boundary conditions have been changed. The cost of creating this DW is the energy difference between both ground states $E' - E$ and is expected to scale with system size as L^y. RG considerations identify this exponent with the θ exponent for droplets. The RG approach aims at describing with scaling laws the behaviour of effective couplings between the degrees of freedom present in the system at increasingly larger length scales L. The DW created in a system of size L is identified with the effective coupling at this length scale. In general, it is expected to scale as L^y, so that, in RG language, y is the dimension of the thermal perturbation. The behaviour of the free-energy close to the $T = 0$ fixed point is, thus, described by the variable TL^{-y}. The sign of y determines whether temperature is a relevant operator or not. If $y < 0$ the perturbation is relevant and $-1/y$ is identified with the correlation length exponent and thus $\theta = y$.

This method allows to create excitations spanning the whole system that are assumed to be typical and give the relevant contribution to the thermodynamics at low temperatures. However, even though DW excitations and droplets are compact objects, the equivalence between these excitations is not clear because it is not evident that the properties of the surface of a closed line (or droplet see Fig. 1.10) are equivalent to those of an open line or DW.

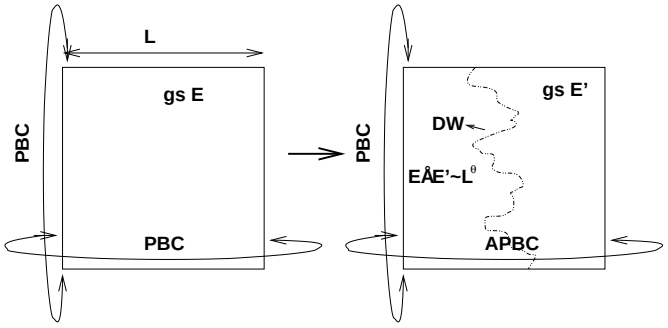

Figure 1.11. Schematic picture of the DW method as described in the text: First we compute the ground state (gs) with PBC along both directions. Then we change to APBC along one direction, the new ground state differs from the old one in the existence of a DW along the direction with PBC. The energy cost of this DW is the energy difference between both gs.

2.4 Dynamics and relation with experiments

In the droplet model the dynamics is governed by the activation over barriers. The equilibrium region grows very slowly in time by annihilation of different droplets. The energy barrier associated to overturning each droplet scales as $B \sim \Upsilon(T)\, L^{\psi}$ with $\theta \leq \psi < d-1$ (see Fig. 1.12). The typical relaxation times are assumed to follow an Arrhenius law [7],

$$t_L = \tau_0 \; e^{\beta \; \Upsilon(T) \; L^{\psi}} \quad . \tag{1.42}$$

Above, τ_0 is a microscopic timescale that we will omit in what follows by considering adimensional times, $t = t'/\tau_0$. Thus, the size of the equilibrium domains grows as $L(t) \propto (\ln t)^{1/\psi}$. The exponential separation between timescales leads naturally to hierarchical dynamics because at different temperatures the active length scales are very different. This is an ingredient in common with the hierarchical models inspired in MFT which have also been proposed to explain the memory and rejuvenation phenomena observed in experiments [BDHV01]. This idea had already been introduced by McMillan [McM84d] who pointed out that at the timescale t only the relaxation of the modes (lengths) whose relaxation times are $\sim t$ are active, while modes corresponding to larger relaxation times seem to be frozen.

Hence, in the droplet picture, the length scales experimentally probed in time t are $L(t)$. Ageing is interpreted as the *non-stationary* effects which arise when the observation time is of the order of the age of the system so that $t/t_w >> 1$ and the size of the dynamically relevant excitations $L(t)$ is of the order of the size of the equilibrium domains, $\xi(t)$, which evolve and age with time. If, on the contrary, the observation time is much smaller

[7] This is the assumption made by Fisher and Huse [FH88b], other authors have assumed a power law dependence of the relaxation times reaching similar conclusions [KH88].

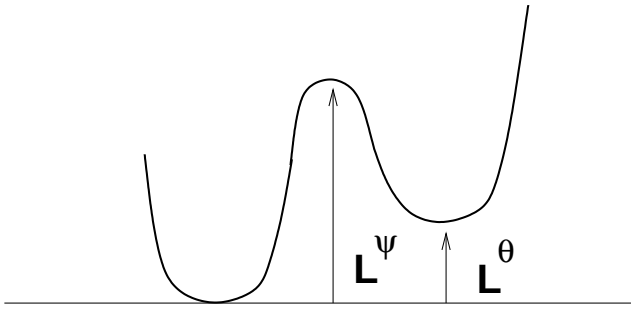

Figure 1.12. Schematic picture of the energy barrier between two configurations $B \sim L^{\psi}$ which differ in a droplet of size L and cost L^{θ}. Note that necessarily $\psi \geq \theta$, since the barrier is always the rate limiting process.

than the age of the system, the dynamics is *stationary* because the system probes the equilibrated regions.

2.4.1 Ageing of the correlation functions: the FDT violation and the connection with glasses

This clear-cut distinction between stationary and non-stationary dynamics is also present in the dynamical solution of mean-field models in the thermodynamic limit [CK93, CK95][8]. The dynamical equations can be solved in the large-time limit assuming the *weak long-term memory* of the system, *i.e.* what happened during the early epochs is not relevant for the large-time dynamics. The solution reveals that the system never reaches true equilibrium at finite times in agreement with the *weak ergodicity breaking scenario* [VHO$^+$96].

Stationary and non-stationary contributions can by disentangled by considering the auto-correlation function,

$$C(t+t_w,t_w) = \frac{1}{V}\sum_i \overline{\langle S_i(t+t_w)S_i(t_w)\rangle_\zeta}. \tag{1.43}$$

where here and henceforth $\langle\cdots\rangle_\zeta$ stands for averaging over the thermal noise or different dynamical histories. We have already seen that in equilibrium, i.e when $t, t_w \to \infty$, the auto-correlation function is equal to $q_{\rm EA}$ (1.1). Here we are interested in the separation between stationary and non-stationary contributions. We can split the autocorrelation function into two parts: $C_{\rm st}$ and $C_{\rm AG}$ as follows,

$$C(t+t_w,t_w) = C_{\rm st}(t) - q_{\rm EA} + C_{\rm AG}(t+t_w,t_w) \ . \tag{1.44}$$

[8]These results have been shown to be valid also for non-disordered systems such as mean-field structural glass models [BM94, MPR94b, FH95, CKPR95].

Where we have defined,

$$C_{\rm st}(t) = \lim_{t_w\to\infty} C(t+t_w,t_w)\,; \qquad \lim_{t\to\infty} C_{\rm st}(t) = q_{\rm EA} \quad , \tag{1.45}$$

and the ageing part is such that,

$$\begin{aligned} \lim_{t\to\infty}\lim_{t_w\to\infty}\ C_{\rm AG}(t+t_w,t_w) &\to q_{\rm EA} \\ \lim_{t\to\infty}\ C_{\rm AG}(t+t_w,t_w) &\to 0 \ . \end{aligned} \tag{1.46}$$

The last equality is a due to the fact that if there is weak ergodicity breaking, a system of a finite age can explore all the other configurations in phase space in a finite observation time. Note that these two correlation functions vary at very different timescales. For $t \ll t_w$ there are only contributions coming from the stationary part and $C > q_{\rm EA}$; whereas if $t \gg t_w$ the main contribution comes from the ageing part $C < q_{\rm EA}$. Thus $C = q_{\rm EA}$ signals the crossover between both regimes.

This separation can be found also for the response function R or its integrated form, the susceptibility: $\chi(t+t_w,t_w) = \int_{t_w}^{t+t_w} R(t+t_w,t')dt'$. The relation between these two quantities is such that the ageing part satisfies the fluctuation-dissipation theorem in a generalised version [CK93, CK95],

$$R_{\rm st}(t) = -\frac{1}{T}\frac{dC_{\rm st}(t)}{dt} \qquad R_{\rm AG}(t_w,t) = \frac{\mathrm{X}(t,t_w)}{T}\ \frac{\partial C_{\rm AG}(t,t')}{\partial t'}\bigg|_{t=t_w} \tag{1.47}$$

Here the $\mathrm{X}(t,t_w)$ is the FDT violation factor. In mean-field models it can be proved that, asymptotically, X depends on both times through the correlation function, so that $\mathrm{X}(t,t_w) = \mathrm{X}\left(C_{\rm AG}(t,t_w)\right)$. In MFT, X depends strongly on the RSB pattern. On the one hand, in models that display full-step RSB at the transition, there are many timescales and X is a non-trivial function of $C_{\rm AG}$. On the other hand, models that can be solved by the one-step RSB ansatz have only one relevant timescale. As a consequence, X takes the constant value m, the size of the blocks in the one-step scheme (1.34), that is a function of temperature. This class of models, to which, p-spin models belong for $p > 2$, are directly linked with the low T behaviour of glasses (see Sec. 1.1). Glasses have only one relevant timescale which governs the out-of-equilibrium dynamics. This phenomenon can be characterised by introducing an effective temperature, $T_{\rm eff} = T/\mathrm{X}(C_{\rm AG})$, so that the usual FDT relation is recovered. Remarkably the similarity between glasses and one-step RSB models goes far beyond: the transition from the liquid to the glass phase in glasses is analogous to the transition by entropic collapse observed in $p-$spin models [pW87, pT87].

2.4.2 Memory, rejuvenation and hierarchical dynamics.

We have seen that any theoretical description of a spin glass must have well separated stationary and non-stationary dynamics, but a consensus in the interpretation of experiments has not yet been reached. The debate has been enhanced by the striking

rejuvenation and memory effects observed in the ageing process upon temperature shifts described in Sec. 1.3.2.

In the droplet context the *chaotic nature* of spin glasses has been advocated to account for the strong rejuvenation observed when cooling the system from T_1 to $T_2 = T_1 - \Delta T$. Provided the time spent at low temperatures is enough to grow an equilibrium length $L = (f(T) \ln t)^{1/\psi}$ larger than the crossover length $l_{\Delta T}$, the ageing process will restart again on cooling the system. On heating back, memory is recovered if there is a large separation between active length scales at each temperature such that the ageing process does not become cumulative [YLB01]. One of the main objections to this interpretation is that it assumes that dynamics is activated. This would result in strong cooling rate effects in the ageing process which are not observed experimentally (see Sec. 1.3.1).

There has been another attempt to interpret these experiments in the absence of chaos: the hierarchical picture. This picture is inspired in the free-energy landscape obtained in MFT which consists in a system of wells within wells hierarchically organised. The idea is to translate this structure to real space and associate to each level in the hierarchy a length scale. As well as in the droplet model, each temperature has a length scale associated so that temperature plays the role of a microscope revealing the finer details of the system [BDHV01]. At T_1 the system is able to equilibrate a region of size L. Because the reconformation of smaller length scales has to proceed before equilibrating bigger domains, the evolution of the domain walls is very slow. On lowering the temperature, shorter length scales fall out-of-equilibrium so that, as long as there is a drastic separation between length scales at T_1 and T_2, one observes the *rejuvenation* associated to the start of the ageing process of these smaller regions. Again, memory is recovered if the time spent at T_2 is not too long so that the typical length scales active at T_1 are not affected .

3. Simulations

Recently, the interplay between experimentalists and theoreticians has led to the ideation of experimental procedures trying to provide evidence of the predictions of different theories [JYN$^+$02b, SVDV02]. For those theoretical predictions that cannot be experimentally checked, one has to make numerical simulations. The use of simulations is ubiquitous in spin glasses since the analytical approach has not yet succeeded to yield any definite conclusion to many problems at both equilibrium and dynamical levels.

Regarding dynamics, one of the main interests is to check whether models reproduce experimental phenomenology or not. Remarkably, the three-dimensional EA model shows ageing in the correlation functions and the susceptibility [Rie93, PRTR01b, PRTR01a]. However, the chaotic and memory effects have not been observed suggesting that maybe the timescales explored are too short [PRTR01b, PRTR01a]. Despite, some of these effects have been reproduced in simulations of the EA in 4 dimensions [BB02].

All the same, these dynamical aspects have been investigated only during the last decade. The main concern has been to work out what is the sound nature of short-ranged spin glasses, trying to decide which of the two more supported pictures, droplet or MFT, describes suitably the low-temperature phase of realistic models. At the root of the rather

contradictory conclusions put forward by several authors are the thermalisation problems present in any spin glass system, due to the existence of a large number of metastable states ($\mathcal{N}_s \sim e^{a V}$) with low energy that prevent the system from exploring the whole phase space in a reasonable time. The impossibility to thermalise large systems at low temperatures raised a long-standing doubt on the relevance that Monte Carlo simulations at finite temperatures have on the low-temperature physics, as numerical results might be affected by critical effects. Currently, it is possible to thermalise modest systems at very low temperatures, thanks to the advance of computer capabilities and of numerical algorithms [KPY01, MMZ00], obtaining results compatible with other methods such as ground state calculations. These results point in the direction that the description of the low-temperature phase is rather a mixture of both pictures droplet and mean field giving rise to the so-called TNT scenario (standing for trivial-non-trivial -see Chap. 4-) [KM00, PY00a]. Still, on the top of it there are the large finite size effects that affect finite dimensional systems so that the final answer is yet to come.

4. Scope of this thesis: excitations, OPF and chaos

Dynamical simulations are less hard because there are no thermalisation problems neither finite-size effects. Then, one may wonder what is the point of investigating the statics of a system whose experimental phenomenology is that of out-of-equilibrium systems. The idea is that the characterisation of excitations through equilibrium properties can give valuable information about the dynamical processes.

The existence of low-lying droplet excitations is typical of many disordered systems including random magnets and disordered manifolds [You98]. The object of this thesis is to investigate several aspects of the typical excitations. In this work we shall try to work out what are the general properties of lowest lying excitations that emerge at finite temperatures.

We have seen that apart from MFT, any description of the low-temperature phase is based on scaling arguments that rely on many unproven assumptions. For this reason many authors have heavily relied upon numerical methods to characterise properly these excitations. The first approach in this direction was the DW method proposed to estimate the thermal exponent, θ. Nowadays, besides the interest of determining the exponent θ, the attention has focused on characterising these excitations not only energetically but also topologically. In this thesis we shall not try to investigate directly typical excitations. Instead we will try to infer their properties from the equilibrium and dynamical behaviour observed at low temperatures.

First we shall focus on the study of order-parameter-fluctuations (OPF). MF spin glasses show strong sample-to-sample fluctuations of the order parameter. This is because in the thermodynamic limit there exist many large scale excitations with finite probability that have a very small overlap with the ground state. In a finite-dimensional system this same situation takes place at least for finite volumes, because large excitations contribute to the OPF at low T with a probability $\sim L^{-\theta}$. Therefore, the analysis of OPF is useful to distinguish between high and low-temperature phases in which large anomalous

excitations come into play. Moreover, from OPF one can get further information about the organisation of these excitations. In MFT we know that different states are related in such a way that the joint distribution of several overlaps fulfils a set of sum rules. Thus, one can measure the lack of self-averageness of the $P(q)$ through these sum rules to learn, in return, about the links between different states. For this reason we have investigated two adimensional parameters that measure these different aspects: the parameter A that remains finite if OPF do not vanish, and, the parameter G, that, in virtue of the sum rules valid in MFT, becomes a step function in the thermodynamic limit: $G = \frac{1}{3}\Theta(T_c - T)$.

The behaviour of OPF at very low temperatures can also be studied from a zero-temperature analysis. This is the spirit of any scaling theory based on RG considerations trying to describe large typical excitations. Here we will follow a different approach to investigate low-temperature properties. It consists in studying first excitations, this is to say *the states closest in energy to the ground state*. In systems such as spin glasses where frustration plays a central role, these low-lying states are scattered in phase space. They can either belong to the ground-state energy valley or to a different energy valley with a small overlap with the ground state. Our main assumption is that this random character of excitations is reflected in the spectrum giving rise to what we call *uncorrelated energy-size scenario*. In this scenario energy gaps between different excitations are independent random variables non-correlated with the size of the excitation. On these grounds, we expect that in the statistics of the lowest excitations is contained the whole information about the low energy states and, in turn, that of typical excitations. The connection between first and typical excitations is made through scaling laws that characterise large size first excitations. Thus, the main interest will be to investigate what low T typical properties can be inferred from these scaling laws.

Finally, we address a different issue concerning the temperature dependence of the free-energy landscape. This is the so-called *chaos* problem. The extreme sensibility of the equilibrium configuration to a temperature change is one of the central assumptions in droplet theory. The concept of chaos had also been introduced in MFT. Since free-energies of different states are random independent variables, the weights of equilibrium states are expected to reshuffle when temperature is changed [MPV87]. The control of the changes of the free-energy landscape at finite temperatures is especially relevant at a dynamical level and recently has attired much attention due to is potential relevance in temperature shift experiments. Here, it is interesting not only to study what are the key ingredients leading to static chaos, but also to work out if rejuvenation effects can be observed in the absence of true static chaos.

5. Summary of the main results

In order to offer a general description of typical excitations a wide number of different models have been analysed. A lot of time is devoted to mean-field models. The analysis of these models is useful because we have a good theoretical control on them so that numerical results for finite systems can be compared with analytical predictions in the thermodynamic limit.

This is especially useful in the study of OPF parameters, for which the behaviour in the thermodynamic limit can be obtained using the Replica Equivalence property. The main outcome of the numerical investigations of parameters measuring OPF is the following:

i) The study of G and A provides a powerful tool to numerically investigate the transition of any spin glass model. This is true even when the sizes studied are small, beyond mean field and also in models without time-reversal symmetry where traditional quantities such as the kurtosis of the overlap distribution, the so-called Binder ratio, do not work.

ii) Numerical investigations support the conjecture that, in any spin-glass model regardless of whether there is RSB or not, $G = 1/3\,\Theta(T_c - T)$ in the large-size limit.

iii) These parameters take *universal* values independent of system size at $T = 0$. The study of lowest lying excitations tells us that this universality is reached under two very mild assumptions: the uniqueness of the ground state and the finite probability of having an excitation with no gap. Furthermore, from the low-temperature behaviour of A we can estimate the value of the thermal exponent θ.

At low temperatures we focus on the analysis of lowest-lying excitations. These are clusters or droplets of volume v and energy cost ϵ that depend on the sample. When the cluster occupies a finite fraction of the total number of spins $v \sim V$, a scaling ansatz can be proposed for the volume and energy distributions. In this situation, the statistics of these large excitations are described by two scaling exponents that we call as *lowest-droplet* exponents: θ_l that accounts for the energy cost of first excitations and λ_l that describes the probability of having a large lowest-lying excitation. The main results are the following:

i) From the statistics of lowest lying excitations we can obtain the θ exponent for droplets that reads $\theta = \theta_l + \lambda_l d$.

ii) The uncorrelated energy-size scenario and its predictions are confirmed by numerical investigations of MF and finite-dimensional models. Within this scenario:

  a) The energy exponent is enough to describe the low-temperature behaviour of energy-related quantities such as the specific heat

  b) Overlap-related quantities such as the $P(q)$ are governed by the thermal exponent θ, so that if $\theta = 0$, there is RSB.

iii) Numerical results reveal that, in finite dimensions, both finite and large-scale excitations yield the same leading contribution to the low T behaviour of any observable.

This last result is linked with the outcome of the study of the chaos and rejuvenation problem in which large and small excitations play different roles.

i) Chaos is a large scale phenomenon, so that, only if low-lying excitations far from the ground state are favoured entropically, a temperature difference can induce the statistical decorrelation of two identical copies of the system.

ii) The rejuvenation of the ageing process is not necessarily associated to the existence of chaos, but to the small scale dynamics. This is the situation met when a temperature change leads to the localisation into the deepest minima of an energy valley. Numerical investigations in a model without chaos, such as the Sinai model, reveal that, in this situation, dynamics at different temperatures involve very different length scales. Therefore, at low temperatures the ageing signal corresponds to explore small excitations that are close in phase space.

This thesis is structured as follows. In chapter 2 we will make a brief overview of the different models that will be analysed during the thesis. The following chapter is devoted to the study of the fluctuations of the order parameter (OPF) and of the parameters measuring them in order to characterise the transition and low-temperature phase of several spin-glass models. The study of the lowest excitations will be addressed in the fourth chapter. There we will see how from the study of lowest excitations one can obtain information about the excitations relevant for the physics at finite temperatures. In chapter 5 we study the chaos problem in different systems with the aim of characterising which are the main ingredients that a chaotic system must contain. And finally, we make detailed numerical simulations to test up to what extent a model with no chaos can reproduce memory and rejuvenation phenomena. In the last chapter we will present the Conclusions that can be drawn from this work. For the sake of simplicity many technical details have been skipped and have been included in several appendices at the end of the thesis.

Chapter 2

MODELS

The main goal of this thesis is to work out what general properties describe excitations in spin glasses. For this reason many different models have been studied analytically and numerically in an attempt to make a unified characterisation of excitations. Usually spin glasses are modelled as a collection of interacting spins with randomly distributed couplings. These spin models have the advantage that allow a description of excitations in energetic and topological terms. Nevertheless, in most of the cases, the numerical approach limits considerably the analysis because only modest system sizes can be well studied.

It is also useful to consider disordered elastic systems. These systems share many of the features of spin glasses including a non-trivial ground state and slow dynamics. However, the presence of elasticity gives a starting point for analytical and numerical studies that is not possible in the spin glass case. This has motivated the study of the directed polymer in random media in $1 + 1$ dimensions (DPRM). A model that, despite its simplicity, is believed to possess many of the subtle properties of glassy systems, and thus it deserves to be called a *baby spin-glass* [Méz90].

A different point of view is that of random potential models. These models describe a spin glass in terms of the statistics of the energy levels, so that only a (free-)energetic characterisation of excitations is possible. We have already seen that the spectrum of excitations in random frustrated systems is very different from that of a ferromagnet in the sense that there exist many large-scale low energy configuration states that contribute to the thermodynamics in the frozen phase. The random model approach offers a much simpler way to analyse this aspect. Moreover, the analytical approach is possible so that it gives complementary information to that obtained from the study of spin models.

In what follows we introduce all the models studied in this thesis.

1. Spin models

The prototypical model for order-disorder transitions in magnetic systems is the Ising model. In this simple model a magnetic system consists of a set of magnetic moments sitting in a cubic lattice of d dimensions. Each magnetic moment is reduced to its z-component so that it is not a vector but a scalar that can take two values $S = \pm 1$. Spins interact with each other via an exchange coupling J_{ij}. The Ising Hamiltonian, thus, reads,

$$\mathcal{H} = -\sum_{ij} J_{ij} S_i S_j - h \sum_i S_i \quad , \tag{2.1}$$

where h is a magnetic field in energy units. Usually the sum is taken over nearest neighbours (nn) pairs, then in the pure case $J_{ij} = J$. For $d > 1$ this model displays a transition into an ordered magnetic phase. The magnetic ordering at low temperatures, depends on the sign of J: $J > 0$ corresponds to ferromagnetic order and the $J < 0$ to antiferromagnetic order.

The importance of this model is that, for its simplicity, it is a model for other non-magnetic order-disorder transitions, *e.g.* lattice gases or binary alloys.

All the spin models studied in this thesis have this same spirit. The analysis of other more specific models, albeit more realistic, would not fit in the general plan of this work. Still, one expects that in the features observed in simple models, most of the physics relevant in real materials is contained. We have investigated, mostly numerically, mean-field as well as short-ranged models.

1.1 Mean Field models: p-spin model

The p-spin model is a generic mean-field model for a spin glass. In this model spins are Ising variables interacting in groups of p spins with $p \geq 2$. It is defined by the following Hamiltonian,

$$\mathcal{H} = -\sum_{i_1 < i_2 \cdots < i_p} J_{i_1 \, \cdots \, i_p} \, S_{i_1} \, \cdots \, S_{i_p} \; - \; h \sum_i S_i \;\; , \qquad S_i = \pm 1 \, , \tag{2.2}$$

where the sum runs over all possible groups of p spins and h is the applied magnetic field. Note that the variance of the distribution of the couplings has to be chosen in order that the energy is extensive, so that for Gaussian couplings it reads ,

$$P(J_{i_1 \, \cdots \, i_p}) = \frac{1}{\sqrt{2 \, \pi \, \sigma^2}} e^{-\frac{J^2_{i_1 \, \cdots \, i_p}}{2 \, \sigma^2}} \, ; \qquad \sigma^2 = \frac{p!}{2 \, V^{p-1}} \tag{2.3}$$

where V is the total number of spins.

1.1.1 Sherrington-Kirkpatrick model

The SK model corresponds to the case $p = 2$ in equation (2.2),

$$\mathcal{H} = -\sum_{i<j} J_{ij} \; S_i \; S_j \; - \; h \sum_i S_i \, ; \qquad S_i = \pm 1 \quad . \tag{2.4}$$

In Sec. 2.2 we have discussed the behaviour when there is no external field: as T is lowered the system has a phase transition at $T_c = 1$ from a paramagnetic phase with $q = 0$ to a SG phase in which TRS and RS are broken [MPV87]. The case with non-zero field is different since as TRS is absent in the Hamiltonian it cannot be broken at the transition. At high temperature, the system is in a ferromagnetic phase with a RS stable solution with $q = q_{\rm EA} \neq 0$. However, at lower temperatures, the symmetric solution is not stable when the system enters the SG phase where RS is broken at infinite step. This transition is continuous in the order parameter and takes place at the point where the eigenvalues of the Hessian matrix vanish. This condition draws a line in the $T - h$ phase diagram known as the de Almeida-Thouless line [dAT78],

$$T = \frac{1}{\sqrt{2\,\pi}} \int dz\; e^{-\frac{1}{2}z^2} \mathrm{sech}^4 \left(\frac{\sqrt{q} z}{T} + \frac{h}{T} \right). \tag{2.5}$$

The transition temperature for each field h can be found numerically using the self-consistency equations for q [MPV87]. The resulting line is displayed in Fig. 2.1. As is schematised in the left panel in Fig. 2.1, below the AT line the $P(q)$ becomes a non-trivial function of q with support in the range $[q_{\rm min}, q_{\rm EA}]$, where $q_{\rm min}$ depends on the applied field.

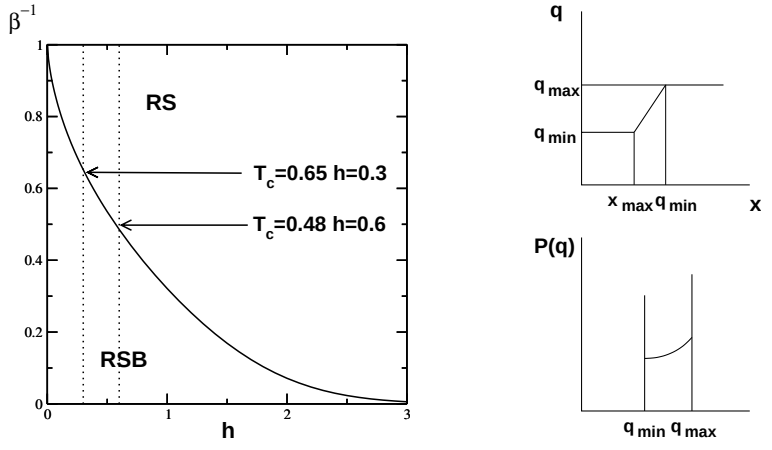

Figure 2.1. AT instability line (2.5). *Left:* Temperature versus magnetic field obtained from solving numerically the de Almeida-Thouless instability condition (2.5). Note that at $h = 0$ $T_c = 1$. The arrows show the transition points corresponding to the parameters used in simulations in Chap. 3, $h = 0.3,\ 0.6$. *Right:* Schematic view of the $q(x)$ and its corresponding $P(q)$ below the AT line.

1.1.2 *p*-spin model, $p = 3$

This model is described by the following Hamiltonian,

$$\mathcal{H} = -\sum_{i_1<i_2<i_3} J_{i_1 i_2 i_3} S_{i_1} S_{i_2} S_{i_3}\,; \qquad S_i = \pm 1. \tag{2.6}$$

We have chosen couplings distributed according to (2.3). Similarly to the SK model in a field, the 3-spin model does not contain TRS in the Hamiltonian. However, the nature of the transition is very different. This transition is discontinuous in the order parameter that jumps from zero to a finite value. The solution below T_c satisfies the one-step RSB ansatz described in Sec. 2.2.1 with $q_0 = 0$. Thus, only the elements of the Q_{ab} matrix in the $m \times m$ diagonal boxes are different from zero.

This is the situation generically met in p-spin models with $p > 2$ [Gar85]. The instability condition $\frac{\partial^2 \mathcal{A}}{\partial Q_{ab} \partial Q_{bc}}\Big|_{Q_{\rm sym}} = 0$ of the high temperature RS solution yields the following expression for the transition temperature in the limit of large p [Gar85],

$$T_c(p) = \frac{1}{2\sqrt{\ln 2}} \left(1 + 2^{1-p} \sqrt{\frac{\pi}{p \left(\ln 2\right)^3}} \right) \quad . \tag{2.7}$$

We have to point out that even though $p = 3$ might seem small the results obtained making this approximation are very accurate, so that we can take $T_c \approx 0.65$ for $p = 3$.

These kind of transitions are driven by a collapse of the configurational entropy (also called entropy crisis) because below T_c the number of states contributing to the partition function become $\mathcal{O}(V)$. These models have been object of a deep study as they have many points in common with the glass transition in structural glasses [pT87, pW87, Méz00]. In particular, it is interesting that the breaking parameter m is directly related to the FDT violation factor in glasses (see Sec. 2.4.1).

These models have also the particularity that at very low temperature the one-step RSB solution becomes also unstable. The stable solution satisfies the full RSB in a similar fashion to that described for the SK model in the presence of a high magnetic field [Gar85].

1.1.3 The spherical Sherrington-Kirkpatrick model

This model is the continuous spin version of the SK model defined above (1.1.1) whose Hamiltonian reads,

$$\mathcal{H} = -\sum_{i<j} J_{ij} \sigma_i \sigma_j \ , \qquad \sum_{i=1}^{V} \sigma_i^2 = V \tag{2.8}$$

Spins are continuous variables $-\infty < \sigma_i < \infty$ that satisfy a global spherical constraint. Couplings are Gaussian distributed variables with zero mean and variance $1/V$.

The properties of the low temperature phase are very different to those of the SK model [KTJ76]. This model can be solved in several ways: using replicas and using the eigenvalue spectrum of a large random matrix and its properties [KTJ76]. At $T_c = 1$ it displays a transition in which the spin configurations condenses on the largest eigenvalue of the spectrum of the coupling matrix. In replica space, the low temperature solution is a marginally stable replica symmetric solution with $Q_{ab} = q_{\rm EA} = 1 - T$. This means that as well as in the SK model the spin-lass susceptibility diverges in the whole low temperature phase but as $V^{1-\alpha}$, $0 < \alpha < 1$.

1.2 Edwards-Anderson model

The Edwards-Anderson (EA) model is the canonical model of a realistic spin glass. We will consider the model without magnetic field. We have V Ising spins sitting on a cubic lattice of size L and dimension d so that $V = L^d$. The Hamiltonian reads (1.12),

$$\mathcal{H} = -\sum_{\langle i,j \rangle} J_{ij} S_i S_j \ , \qquad S_i = \pm 1 \quad . \tag{2.9}$$

where couplings are Gaussian with a variance $\mathcal{O}(1)$. The interaction is short range, so that usually one spin interacts with its $2d$ nearest neighbours. In this analysis, we have also considered the $d = 3$ model (3d nnn) where spins interact with the nearest and next nearest neighbours, i.e. one spin interacts with 26 spins instead of 6 spins. The reason for this is that we expect it to have qualitatively the same features as the 3d model but with fewer thermalisation problems and smaller finite-size effects.

As we have already noted, theoretically very few is known about models with finite d. The upper critical dimension above which the MF description is expected to hold is $ucd = 6$ [FH91a]. For lower dimensions apart from the Ising chain ($d = 1$) that can be solved analytically, only scaling arguments that do not come from microscopic considerations can try to account for the behaviour of such models at low temperature. One of the main issues to which many studies have been devoted is the determination of the lower critical dimension. It is well known that the for $d = 1$ the transition is at $T = 0$ [BM85]. In the literature [McM84c, BM84, BY88, KHS92, RSB$^+$96b], many authors have reported that this is also the case also for the two-dimensional Ising spin glass. The first DW calculations yielded a positive θ in the 3d implying that there was a transition at finite temperature [BM84]. However, due to the large finite-size effects present at criticality, the characterisation of the transition point has only been possible very recently [MPRL98a, BCF$^+$00].

2. The directed polymer in random media

The DPRM belongs to the wide class of elastic manifolds in random media [MP91, BF93, BBM96, GD94, GD95, CGD00, SA00] which describes a wide range of physically interesting systems such as the domain walls of ferromagnets with weak bond randomness [HH85] and vortex lattice systems with weak random-periodic pinning centres [FL78, Grü88, GD94]. We will address the DPRM in $1 + 1$ dimensions which is described by the following Hamiltonian in the continuous limit,

$$H_0[V, h, \phi] = \int_0^L dz \left[\frac{\kappa}{2} \left(\frac{d\phi(z)}{dz} \right)^2 + V_0(\phi(z), z) \right] . \tag{2.10}$$

The scalar field ϕ is a single valued function (*i.e. oriented.* objects with no overhangs are considered) and stands for the displacement of the elastic object at point z in a one-dimensional internal space of size L. An example of the ground state configuration and an excited state is shown in Fig. 2.2. The 1st term in the Hamiltonian is the elastic energy,

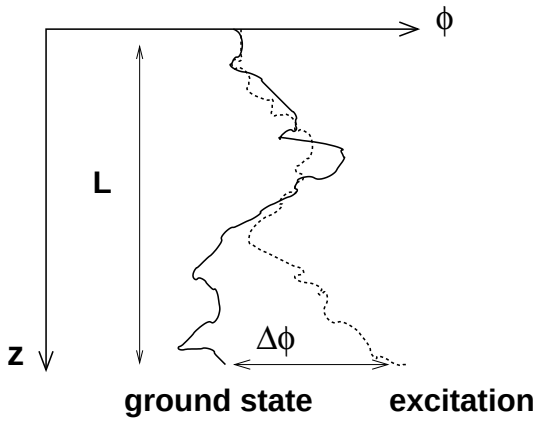

Figure 2.2. DPRM: example of the configuration of the ground state (minimum energy) and the lowest lying excitation for a given realisation of the quenched disorder. Note that $\phi(z = L)$ is the transversal coordinate of the endpoint of a DP of 'length' L.

κ being the elastic constant. The random pinning medium is modelled by the quenched random potential $V_0(\phi, z)$ with zero mean and short-ranged spatial correlation,

$$\overline{V_0(\phi, z)} = 0\,; \qquad \overline{V_0(\phi, z)V_0(\phi', z')} = 2D\delta(\phi - \phi')\delta(z - z') \tag{2.11}$$

The main interest is that many exact results are known from this model [HHZ95], and thus we have a good control of excitations at all levels that can yield valuable hints for the analysis of more complex spin-glass models. It is in the frozen phase at all finite temperatures in the sense that its scaling properties are always governed by the $T = 0$ glassy fixed point. The interest of this model relies on the existence of anomalously large excitations with a low free-energy cost $\sim L^\theta$, $\theta = 1/3$ that bring about very large (extensive with L) fluctuations of the ground-state end point position $\Delta\phi$. This is the simplest version of an excitation in a random disordered from which many information can be obtained because the theoretical analysis is much easier.

3. Random potential models

The random potential models are, in general, models that only provide an energetic description of the system. Originally, random potential models have been defined by the statistics of the energy levels $\{\epsilon_i\}$ given by a distribution $\mathcal{P}(\{\epsilon_i\})$ without any specification netiher on dynamics nor on spatial effects. We will also consider models in one dimension where dynamical rules can be put by hand, so that to each site in a one dimensional box we can associate an energy drawn from the probability distribution.

3.1 The random energy (exponential) model

The REM is one of the simplest models of a spin-glass. It was introduced by Derrida [Der81] in an attempt to describe a spin glass only by looking at the statistics of the energy levels. This model is defined by a set of 2^V configurations which are drawn from a Gaussian distribution,

$$P(E) = \frac{1}{\sqrt{\pi\, V}} e^{\frac{-E^2}{V}} \quad . \tag{2.12}$$

In this model the different energy levels are uncorrelated, so that the joint probabilities factorise,

$$P(E_1, E_2) = P(E_1)P(E_2) \quad , \tag{2.13}$$

implying that all the information is contained in the statistics of a single level. A priori, this was supposed to describe the level statistics in mean-field models. However, as pointed out by Derrida, for any generic random p-spin model (2.2) this property only holds strictly in the limit $p \to \infty$. Nevertheless, the analysis of the $p-$spin model reveals that the convergence to the REM is very fast and that possibly the low T behaviour for $p > 2$ is similar to the $p \to \infty$ behaviour [GM81, Rie92].

This model is solvable analytically. A saddle point equation yields that the average energy for large V reads $\overline{E} = -\beta\, \frac{V}{2}$, where $\overline{(\cdots)}$ stands for the average over the energy levels distribution (2.12). From the expression of the entropy,

$$\overline{S(T)} = V \left(\ln 2 - \frac{\overline{E}^2}{V^2} \right) \tag{2.14}$$

it follows that we observe that at $T_f = \left(2\sqrt{\ln 2}\right)^{-1}$ the entropy vanishes. Since this is a discrete model the entropy cannot be negative, therefore below T_f the system is frozen into the last available state $E_0 = -\frac{V}{2\,T_f}$ and the entropy is zero so that the specific heat in this model vanishes below T_f. This kind of transitions where entropy vanishes and there are a finite number of states which contribute to the partition function is said to be driven by an *entropy collapse*. This is precisely the mechanism described above that leads to the transition in p-spin systems for $p > 2$ [1].

In replica space these transitions are discontinuous in the order parameter q, which at the transition jumps from zero to a finite value q_{EA}, and thus are different from the transition displayed by the SK model which is continuous in the order parameter. Gross and Mézard solved the $p \to \infty$ random p-spin to find that below T_f replica symmetry was broken in the most simplest way according to the Parisi ansatz: i.e. a one-step RSB, so that the overlap between states could have only two possible values [GM81]. In the TAP approach this discontinuous character is reflected too in the number of solutions

[1] Note that $T_f = \left(2\sqrt{\ln 2}\right)^{-1}$ is precisely the transition temperature obtained by taking the infinite p limit in expression (2.7).

($\mathcal{N}_s$) of the self-consistency equations for the local magnetisations. In the $p \to \infty$ limit at T_c there is a jump from $\mathcal{N}_s = 1$ corresponding to the single solution of the PM phase to $\mathcal{N}_s = 2^V$. For p finite, $\mathcal{N}_s$ is also discontinuous and jumps from one to $\mathcal{N}_s(p) < e^{\alpha(p)V}$ with $\alpha(p)$ not very far from $\ln 2$ [Rie92].

In the large-V limit, the number of states above the treshold E_0 increases exponentially $\mathcal{N}_s = \exp\left[2\sqrt{\ln 2}\,(E - E_0)\right]$. Thus in order to have a finite entropy, levels which contribute significantly to the partition function will be close in energy to E_0 such that energy differences will be very small $\epsilon = E - E_0 = \mathcal{O}(1)$.

Our interest will be to study the properties at low temperatures. The low-temperature phase of the REM can be shown to be equivalent to that of the trap model [BM97] in which enery states are chosen according to an exponential probability distribution,

$$P(\epsilon) = \frac{1}{T_f} e^{-\frac{|\epsilon|}{T_f}} \tag{2.15}$$

where ϵ has been chosen to be negative. This is what we will call random energy exponential model (REEM). Interestingly, in the trap model, the dynamical counterpart of the entropy collapse is the ageing due to the very long times spent in the deepest minima of the potential.

3.2 The Sinai model

We have also studied the Sinai model in one dimension [Sin81]. This model describes the dynamics of a particle under the action of a random force $F(x)$ which models a disordered medium [BCGlD90]. In general, this is a toy model for a wide range of physical systems in which activated dynamics over energy barriers play an important role such as the movement of domain walls or dynamics of dislocations. Recently, this model was argued to be relevant to describe the unzipping transition of DNA [LN01]. In our case we are interested in studying the motion of the pining centre of a domain wall in a spin glass. In such a system, different domain wall conformations of low energy are separated by energy barriers. In this very simplified one-dimensional model, each site corresponds to a different state or configuration with energy $V(x)$, where x stands for the phase space coordinate. The Sinai potential is a Random Walk in phase space that has long range correlations so that energy barriers grow proportionally to the distance,

$$\overline{(V(x) - V(y))^2} = \sigma\,|x - y| \quad . \tag{2.16}$$

Therefore in contrast to the REM, the potentials at different sites are correlated. This model, as well as the DPRM, has no thermodynamic transition. All the thermodynamics is governed by the absolute minimum and the fluctuations around it. The interest of this model is that it is explicitly hierarchical because the structure of the random potential is strictly self-similar and therefore it is very useful to see what is the effect of this structure of phase space on the dynamics and specially on the rejuvenation and memory effects observed experimentally.

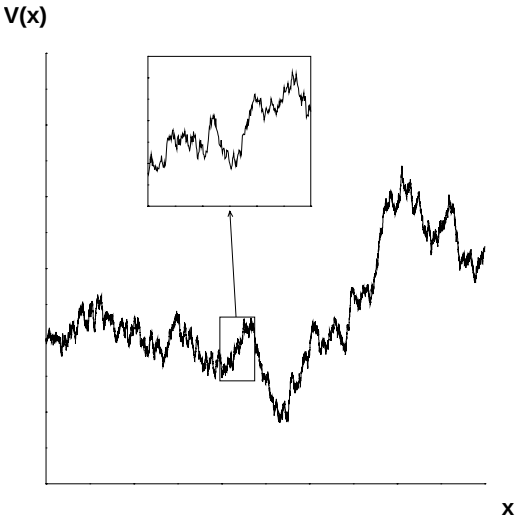

Figure 2.3. Sinai potential: example of a sample of the random potential where x is the position in phase space. In the box we plot the amplification of the selected region to show the self-affine character of the potential .